
On the Similarity between the Laplace and Neural Tangent Kernels

Amnon Geifman¹

Abhay Yadav²

Yoni Kasten¹

Meirav Galun¹

David Jacobs²

Ronen Basri¹

¹Department of Computer Science, Weizmann Institute of Science, Rehovot, Israel

²Department of Computer Science, University of Maryland, College Park, MD

Abstract

Recent theoretical work has shown that massively overparameterized neural networks are equivalent to kernel regressors that use *Neural Tangent Kernels* (NTK). Experiments show that these kernel methods perform similarly to real neural networks. Here we show that NTK for fully connected networks is closely related to the standard Laplace kernel. We show theoretically that for normalized data on the hypersphere both kernels have the same eigenfunctions and their eigenvalues decay polynomially at the same rate, implying that their Reproducing Kernel Hilbert Spaces (RKHS) include the same sets of functions. This means that both kernels give rise to classes of functions with the same smoothness properties. The two kernels differ for data off the hypersphere, but experiments indicate that when data is properly normalized these differences are not significant. Finally, we provide experiments on real data comparing NTK and the Laplace kernel, along with a larger class of γ -exponential kernels. We show that these perform almost identically. Our results suggest that much insight about neural networks can be obtained from analysis of the well-known Laplace kernel, which has a simple closed form.

1 Introduction

Neural networks with significantly more parameters than training examples have been successfully applied to a variety of tasks. Somewhat contrary to common wisdom, these models typically generalize well to unseen data. It has been shown that in the limit of infinite model size, these neural networks are equivalent to kernel regression using a family of novel *Neural Tangent Kernels* (NTK) [27, 1, 2]. NTK methods can be analyzed to explain many properties of neural networks in this limit, including their ability to generalize [9, 10, 14, 31]. Recent experimental work has shown that in practice, kernel methods using NTK perform similarly, and in some cases better, than neural networks [5], and that NTK can be used to accurately predict the dynamics of neural networks [1, 2, 8].

These results raise an important question: Is NTK significantly different from standard kernels? For the case of fully connected (FC) networks, [5] provides experimental evidence that NTK is especially effective, showing that it outperforms the Gaussian kernel on a large suite of machine learning problems. Consequently, they argue that NTK should be added to the standard machine learning toolbox. [10] has shown empirically that the dynamics of neural networks on randomly labeled data more closely resembles the dynamics of learning through stochastic gradient descent with the Laplace kernel than with the Gaussian kernel. In this paper we show theoretically and experimentally that NTK does closely resemble the Laplace kernel, already a standard tool of machine learning.

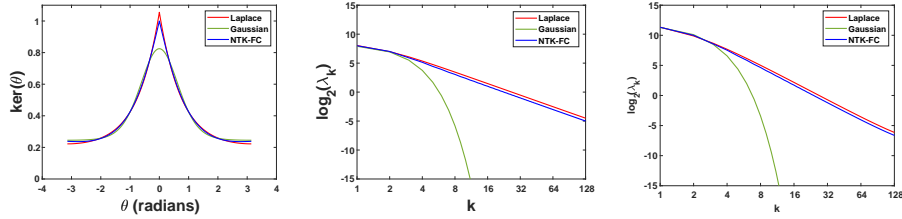


Figure 1: Left: An overlay of the NTK for a FC network with 6 layers with the Laplace and Gaussian kernels, as a function of the angle between their arguments. The exponential kernels are modulated by an affine transformation to achieve a least squares fit to the NTK. Note the high degree of similarity between the Laplace kernel and NTK. Middle: eigenvalues as a function of frequency in \mathbb{S}^1 . The slopes in these log-log plots indicate the rate of decay, which is similar for both the Laplace kernel and for NTK for FC of 6 layers. (Empirical slopes are -1.94 for both the Laplace and NTK-FC.) The eigenvalues of the Gaussian kernel, in contrast, decay exponentially. Right: Same in \mathbb{S}^2 . (Empirical slopes are -2.75 for the Laplace and NTK-FC.)

Kernels are mainly characterized by their corresponding Reproducing Kernel Hilbert Space (RKHS), which determines the set of functions they can produce. They are further characterized by the RKHS norm they induce, which is minimized (implicitly) in every regression problem. Our main result is that when restricted to the hypersphere \mathbb{S}^{d-1} , NTK for a FC network with bias has the same RKHS as the Laplace kernel, defined as $k^{\text{Lap}}(\mathbf{x}, \mathbf{z}) = e^{-c\|\mathbf{x}-\mathbf{z}\|}$ for points $\mathbf{x}, \mathbf{z} \in \mathbb{S}^{d-1}$ and constant $c > 0$. This is shown by establishing that the eigenvalues of NTK and the Laplace kernels decay at the same rate (see Figure 1), implying in turn that gradient descent (GD) with both kernels should have the same dynamics, explaining [10]’s experiments. In previous work, the eigenfunctions and eigenvalues of NTK have been derived on the hypersphere for networks with only one hidden layer, while these properties of the Laplace kernel have been studied in \mathbb{R}^d . We derive new results for the Laplace kernel on the hypersphere, and for NTK for deep networks on the hypersphere and in \mathbb{R}^d . In \mathbb{R}^d , NTK gives rise to radial eigenfunctions, forgoing the shift invariance property of exponential kernels. Experiments indicate that this difference is not significant in practice.

Finally, we show experiments indicating that the Laplace kernel achieves similar results to those obtained with NTK on real-world problems. We further show that by using the more general, γ -exponential kernel [40], which allows for one additional parameter, $k^\gamma(\mathbf{x}, \mathbf{z}) = e^{-c\|\mathbf{x}-\mathbf{z}\|^\gamma}$, we achieve slightly superior performance to NTK on a number of standard datasets.

2 Related Works

The connection between neural networks and kernel methods has been investigated for over two decades. Early work considered networks of infinite width initialized randomly in which only the last layer is trained, and showed that these are equivalent to Gaussian Processes (GP) [46, 37], where training can be used to achieve exact Bayesian inference with a GP prior. In this context, [17] introduced the Arc-cosine kernel, while [20] showed a duality between neural networks and compositional kernels.

More recent work introduced the family of neural tangent kernels (NTK) [27, 1, 2]. This work showed for massively overparameterized and fully trained networks, that their training dynamics closely follow the path of kernel gradient descent, and that training converges to the solution of kernel regression with NTK. Follow-up work defined analogous kernels for residual [26] and convolutional networks [2, 30]. Recent work also showed empirically that classification with NTK achieves performance similar to deep neural networks with the corresponding architecture [2, 30].

The equivalence between kernels and overparameterized neural networks opened the door to studying inductive bias in neural networks. For two layer, FC networks, [6, 8, 15] investigated the spectral property of the NTK when the data is distributed uniformly on the hypersphere, showing in particular that with GD low frequencies are learned before higher ones. [7] extended these results to non-uniform distributions. [47] analyzed the eigenvalues of NTK over the Boolean cube, and [22] analyzed its spectrum under approximate pairwise orthogonality. [6, 12] further leveraged the spectral properties of the kernels to investigate their RKHS in the case of bias free two layer networks. Our results apply to deep networks with bias. [25] studied approximation bounds for two layer neu-

ral networks, and [9, 10, 14, 31] studied generalization properties of kernel methods in the context of neural networks.

Positive definite kernels and their associated RKHSs have been studied extensively, see, e.g., [42, 44] for reviews. The spectral properties of classic kernels, e.g., the Gaussian and Laplace kernels, are typically derived for input in \mathbb{R}^d [29]. Several papers examine the RKHS of common kernels (e.g., the Gaussian and polynomial) on the hypersphere [34, 35, 36].

Recent work compares the performance of NTK to that of common kernels. Specifically, [5]’s experiments suggest that NTK is superior to the Gaussian and low degree polynomial kernels. [10] compares the learning speed of GD for randomly mislabeled data, showing that NTK learns such data as fast as the Laplace kernel and much faster than the Gaussian kernel. Our analysis provides a theoretical justification of this result.

3 NTK vs. the Exponential Kernels

Our aim is to compare NTK to common kernels. In comparing kernels we need to consider two main properties: first, what functions are included in their respective RKHS and secondly, how their respective norms behave. (These concepts are reviewed below in Sec. 3.1.) The answer to the former question determines the set of functions considered for regression, while the answer to the latter determines the result of regression. Together, these will determine how a kernel generalizes to unseen data points. Below we see that on the hypersphere both NTK and exponential kernels (e.g., Gaussian and Laplace) give rise to the same set of eigenfunctions. Therefore, the answers to the questions above are determined fully by the corresponding eigenvalues. Moreover, the asymptotic decay rate of the eigenvalues of each kernel determines their RKHS.

As an example consider the exponential kernels in \mathbb{R}^d , i.e., the kernels $e^{-c\|\mathbf{x}-\mathbf{z}\|^\gamma}$, where $c > 0$ and $0 < \gamma \leq 2$ [40]. These shift invariant kernels have the Fourier transform as their eigenfunctions. The eigenvalues of the Gaussian kernel, i.e., $\gamma = 2$, decay exponentially, implying that its respective RKHS includes only infinitely smooth functions. In contrast, the eigenvalues of the Laplace kernel, i.e., $\gamma = 1$, decay polynomially, forming a space of continuous, but not necessarily smooth functions.

Our main theoretical result is that when restricted to the hypersphere \mathbb{S}^{d-1}

$$\mathcal{H}^{\text{Gauss}} \subset \mathcal{H}^{\text{Lap}} = \mathcal{H}^{\text{FC}_\beta(2)} \subseteq \mathcal{H}^{\text{FC}_\beta(L)},$$

where $\mathcal{H}^{\text{Gauss}}$ and \mathcal{H}^{Lap} denote the RKHSs associated with the Gaussian and Laplace kernels, and $\mathcal{H}^{\text{FC}_\beta(L)}$ denotes the NTK for a FC network with L layers and bias. Further empirical results indicate that $\mathcal{H}^{\text{Lap}} = \mathcal{H}^{\text{FC}_\beta(L)}$ for the entire range $L \geq 2$.

Next we briefly recall basic concepts in kernel regression. We subsequently characterize the RKHS of NTK and the Laplace kernel and show their equivalence in \mathbb{S}^{d-1} . Finally, we discuss how these kernels extend outside of the sphere to the entire \mathbb{R}^d space. All lemmas and theorems are proved in the supplementary material.

3.1 Preliminaries

We consider positive definite kernels $\mathbf{k} : \mathcal{X} \times \mathcal{X} \rightarrow \mathbb{R}$ defined over a compact metric space \mathcal{X} endowed with a finite Borel measure \mathcal{V} . Such kernels are associated with a Reproducing Kernel Hilbert Space (RKHS) of functions, \mathcal{H} , which includes the set of functions the kernel reproduces, i.e., $f(\mathbf{x}) = \langle f, \mathbf{k}(\cdot, \mathbf{x}) \rangle_{\mathcal{H}}$ where the inner product is inherited from the respective Hilbert space. According to Mercer’s theorem \mathbf{k} can be written as

$$\mathbf{k}(\mathbf{x}, \mathbf{z}) = \sum_{i \in I} \lambda_i \Phi_i(\mathbf{x}) \Phi_i(\mathbf{z}), \quad \mathbf{x}, \mathbf{z} \in \mathcal{X}, \quad (1)$$

where $\{(\lambda_i, \Phi_i)\}_{i \in I}$ are the eigenvalues and eigenfunctions of \mathbf{k} with respect to the measure \mathcal{V} , i.e.,

$$\int k(\mathbf{x}, \mathbf{z}) \Phi_i(\mathbf{z}) d\mathcal{V}(\mathbf{z}) = \lambda_i \Phi_i(\mathbf{x}).$$

The RKHS \mathcal{H} is the space of functions $f \in \mathcal{H}$ of the form $f(\mathbf{x}) = \sum_{i \in I} \alpha_i \Phi_i(\mathbf{x})$ whose RKHS norm is finite, i.e., $\|f\|_{\mathcal{H}} = \sum_{i \in I} \frac{\alpha_i^2}{\lambda_i} < \infty$. The latter condition restricts the set of functions in an RKHS, allowing only functions that are sufficiently smooth in accordance with the asymptotic decay of λ_k .

The literature considers many different kernels (see, e.g., [24]). Here we discuss the family of γ -exponential kernels $\mathbf{k}^\gamma(\mathbf{x}, \mathbf{z}) = e^{-c\|\mathbf{x}-\mathbf{z}\|^\gamma}$, $0 < \gamma \leq 2$, which include the Laplace ($\gamma = 1$) and the Gaussian ($\gamma = 2$) kernels.

Neural Tangent Kernel. Let $f(\theta, \mathbf{x})$ denote a neural network function with trainable parameters θ . Then the corresponding NTK is defined as

$$\mathbf{k}^{\text{NTK}}(\mathbf{x}, \mathbf{z}) = \mathbb{E}_{\theta \sim \mathcal{P}} \left\langle \frac{\partial f(\theta, \mathbf{x})}{\partial \theta}, \frac{\partial f(\theta, \mathbf{z})}{\partial \theta} \right\rangle,$$

where expectation is taken over the probability distribution \mathcal{P} of the initialization of θ , and we assume that the width of each layer tends to infinity. Our results focus on NTK kernels corresponding to deep, fully connected network architectures that may or may not include bias, where bias, if it exists, is initialized at zero. We denote these kernels by $\mathbf{k}^{\text{FC}_0(L)}$ for the bias free version and $\mathbf{k}^{\text{FC}_\beta(L)}$ for NTK with bias and define them in the supplementary material.

Kernel regression. Given training data $\{(\mathbf{x}_i, y_i)\}_{i=1}^n$, $\mathbf{x}_i \in \mathcal{X}$, $y_i \in \mathbb{R}$, kernel regression is formulated as

$$\min_{f \in \mathcal{H}} \|f\|_{\mathcal{H}} \quad \text{s.t.} \quad \forall i, f(\mathbf{x}_i) = y_i. \quad (2)$$

The solution satisfies $f(\mathbf{x}) = \mathbf{k}_{\mathbf{x}}^T K^{-1} \mathbf{y}$, where the entries of $\mathbf{k}_{\mathbf{x}} \in \mathbb{R}^n$ are $\mathbf{k}(\mathbf{x}, \mathbf{x}_i)$, K is the $n \times n$ matrix with $K_{ij} = \mathbf{k}(\mathbf{x}_i, \mathbf{x}_j)$ and $\mathbf{y} = (y_1, \dots, y_n)^T$.

3.2 NTK in \mathbb{S}^{d-1}

We next consider the NTK for fully connected networks applied to data restricted to the hypersphere \mathbb{S}^{d-1} . To characterize the kernel, we first aim to determine the eigenvectors of NTK. This will be a direct consequence of Lemma 1. Subsequently in Theorem 1 we will characterize the decay rate of the corresponding eigenvalues.

Lemma 1. *Let $\mathbf{k}^{\text{FC}_\beta(L)}(\mathbf{x}, \mathbf{z})$, $\mathbf{x}, \mathbf{z} \in \mathbb{S}^{d-1}$, denote the NTK kernels for FC networks with $L \geq 2$ layers, possibly with bias initialized with zero. This kernel is zonal, i.e., $\mathbf{k}^{\text{FC}_\beta(L)}(\mathbf{x}, \mathbf{z}) = \mathbf{k}^{\text{FC}_\beta(L)}(\mathbf{x}^T \mathbf{z})$. (Note the abuse of notation, which should be clear by context.)*

We note that for the bias-free $\mathbf{k}^{\text{FC}_0(L)}$ this lemma was proven in [7] and we extend the proof to allow for bias. It is well known that the spherical harmonics are eigenvectors for any zonal kernel with respect to the uniform measure on \mathbb{S}^{d-1} with $d \geq 3$. Therefore, due to Mercer's Theorem (1), any zonal kernel \mathbf{k} can be written as

$$\mathbf{k}(\mathbf{x}, \mathbf{z}) = \sum_{k=0}^{\infty} \lambda_k \sum_{j=1}^{N(d,k)} Y_{k,j}(\mathbf{x}) Y_{k,j}(\mathbf{z}), \quad (3)$$

where $Y_{k,j}(\cdot)$ denotes the spherical harmonics of \mathbb{S}^{d-1} , $N(d, k)$ denotes the number of harmonics of order k in \mathbb{S}^{d-1} , and λ_k are the respective eigenvalues. On the circle \mathbb{S}^1 the eigenvectors are the Fourier series, and $\mathbf{k}(\mathbf{x}, \mathbf{z}) = \sum_{k=0}^{\infty} \frac{1}{c_k} \lambda_k \cos(k\theta)$, where $\theta = \arccos(\mathbf{x}^T \mathbf{z})$ and c_k is a normalization factor, $c_0 = 4\pi^2$ and $c_k = \pi^2$ when $k \geq 1$.

Deriving the eigenvalues for NTK for deep networks is complicated, due to its recursive definition. For a two-layer network without bias, [6, 12] proved that the eigenvalues decay at a rate of $O(k^{-d})$. With no bias, however, two-layer networks are nonuniversal, and in particular $\lambda_k = 0$ for odd $k \geq 3$ [8]. To avoid this issue Theorem 1 establishes that with bias NTK is universal for any number of layers $L \geq 2$, and its eigenvalues decay at a rate no faster than $O(k^{-d})$. Moreover, with $L = 2$ the eigenvalues decay exactly at the rate of $O(k^{-d})$.

Theorem 1. *Let $\mathbf{x}, \mathbf{z} \in \mathbb{S}^{d-1}$. With bias initialized at zero:*

1. $\mathbf{k}^{\text{FC}_\beta(L)}$ decomposes according to (3) with $\lambda_k > 0$ for all $k \geq 0$, and
2. $\exists k_0$ and constants $C_1, C_2, C_3 > 0$ that depend on the dimension d such that $\forall k > k_0$
 - (a) $C_1 k^{-d} \leq \lambda_k \leq C_2 k^{-d}$ if $L = 2$, and
 - (b) $C_3 k^{-d} \leq \lambda_k$ if $L \geq 3$.

The proof of this theorem relies mainly on showing that the algebraic operations in the recursive definition of NTK (including addition, product and composition) do not increase the rate of decay. The consequence of Theorem 1 is that NTK for FC networks gives rise to an infinite size feature space and that its eigenvalues decay no faster than $O(k^{-d})$. While our proofs only establish a bound for the case that $L \geq 3$, empirical results suggest that the eigenvalues for these kernels decay exactly as $\Theta(k^{-d})$, as can be seen in Figure 1.

3.3 NTK vs. exponential kernels in \mathbb{S}^{d-1}

The polynomial decay of the eigenvalues of NTK suggests that NTK is closely related to the Laplace kernel, as we show next. Indeed, any shift invariant and isotropic kernel, i.e., $\mathbf{k}(\mathbf{x}, \mathbf{y}) = \mathbf{k}(\|\mathbf{x} - \mathbf{y}\|)$, in \mathbb{R}^d is zonal when restricted to the hypersphere, since $\mathbf{x}, \mathbf{y} \in \mathbb{S}^{d-1}$ implies $\|\mathbf{x} - \mathbf{y}\|^2 = 2(1 - \mathbf{x}^T \mathbf{y})$. Therefore, in \mathbb{S}^{d-1} the spherical harmonics are the eigenvectors of the exponential kernels.

[34] shows that the Gaussian kernel yields eigenvalues that decay exponentially fast. In contrast we next prove that the eigenvalues of the Laplace kernel restricted to the hypersphere decay polynomially as $\Theta(k^{-d})$, the same decay rate shown for NTK in Theorem 1 and in Figure 1.

Theorem 2. Let $\mathbf{x}, \mathbf{z} \in \mathbb{S}^{d-1}$ and write the Laplace kernel as $\mathbf{k}^{\text{Lap}}(\mathbf{x}^T \mathbf{z}) = e^{-c\sqrt{1-\mathbf{x}^T \mathbf{z}}}$, restricted to \mathbb{S}^{d-1} . Then \mathbf{k}^{Lap} can be decomposed as in (3) with the eigenvalues λ_k satisfying $\lambda_k > 0$, and $\exists k_0$ such that $\forall k > k_0$ it holds that:

$$B_1 k^{-d} \leq \lambda_k \leq B_2 k^{-d}$$

where $B_1, B_2 > 0$ are constants that depend on the dimension d and the parameter c .

Our proof uses the decay rate of the Laplace kernel in \mathbb{R}^d , and results due to [36, 35] that relate Fourier expansions in \mathbb{R}^d to their corresponding spherical harmonic expansions in \mathbb{S}^{d-1} . This allows us to state our main theoretical result.

Theorem 3. Let \mathcal{H}^{Lap} denote the RKHS for the Laplace kernel restricted to \mathbb{S}^{d-1} , and let $\mathcal{H}^{\text{FC}_\beta(L)}$ denote the NTK corresponding respectively to a FC network with L layers with bias, restricted to \mathbb{S}^{d-1} , then $\mathcal{H}^{\text{Lap}} = \mathcal{H}^{\text{FC}_\beta(2)} \subseteq \mathcal{H}^{\text{FC}_\beta(L)}$.

The common decay rates of NTK and the Laplace kernel in \mathbb{S}^{d-1} imply that the set of functions in their RKHSs are identical, having the same smoothness properties. In particular, due to the norm equivalence of RKHSs and Sobolev spaces both spaces include functions that have weak derivatives up to order $d/2$ [36]. We recall that empirical results suggest further that $\mathbf{k}^{\text{FC}_\beta(L)}$ decays exactly as $\Theta(k^{-d})$, and so we conjecture that $\mathcal{H}^{\text{Lap}} = \mathcal{H}^{\text{FC}_\beta(L)}$. We note that despite this asymptotic similarity, the eigenvalues of NTK and the Laplace kernel are not identical even if we correct for shift and scale. Consequently, each kernel may behave slightly differently. Our experiments in Section 4 suggest that this results in only small differences in performance.

The similarity between NTK and the Laplace kernel has several implications. First, the dynamics of gradient descent for both kernels [16] should be similar. For a kernel with eigenvalues $\{\lambda_i\}_{i=1}^\infty$ a standard calculation shows that GD requires $O(1/\lambda_i)$ time steps to learn the i th eigenfunction (e.g., [3, 8]). For both NTK and the Laplace kernel in \mathbb{S}^{d-1} this implies that $O(k^d)$ time steps are needed to learn a harmonic of frequency k . This is in contrast for instance with the Gaussian kernel, where the time needed to learn a harmonic of frequency k grows exponentially with k . This in particular explains the empirical results of [10], where it was shown that fitting noisy class labels with the Laplace kernel or neural networks requires a similar number of SGD steps. The authors of [10] conjectured that ‘‘optimization performance is controlled by the type of non-smoothness,’’ as indeed is determined by the identical RKHS for NTK and the Laplace kernel.

The similarity between NTK and the Laplace kernel also implies that they have similar generalization properties. Indeed various generalization bounds rely explicitly on spectral properties of kernels.

For example, given a set of training points $X \subseteq \mathbb{S}^{d-1}$ and a target function $f : \mathbb{S}^{d-1} \rightarrow \mathbb{R}$, then the error achieved by the kernel regression estimator given X , denoted \hat{f}_X , is (see, e.g., [28])

$$\|f - \hat{f}_X\|_\infty \leq C \cdot h(X)^\alpha \|f\|_{\mathcal{H}_k}, \quad f \in \mathcal{H}_k$$

where $h(X) := \sup_{\mathbf{z} \in \mathbb{S}^{d-1}} \inf_{\mathbf{x} \in X} \arccos(\mathbf{z}^T \mathbf{x})$ is the mesh norm of X and α depends on the smoothness property of the kernel. Specifically, for both the Laplace kernel and NTK $\alpha = 1/2$.

Likewise, with n training points and $f \in \mathcal{H}_k$, [33] derived the following lower bound

$$\mathbb{E}_X \left((f - \hat{f}_X)^2 \right) \geq \sum_{i=n+1}^{\infty} \alpha_i$$

Where α_i are the eigenvalues of f . Both of these bounds are equivalent asymptotically up to a constant for NTK (with bias) and the Laplace kernel.

3.4 NTK vs. common kernels in \mathbb{R}^d

While theoretical discussions of NTK largely assume the input data is normalized to lie on the sphere, such normalization is not the common practice in neural network applications. Instead, most often each feature is normalized separately by setting its mean to zero and variance to 1. Other normalizations are also common. It is therefore important to examine how NTK behaves outside of the hypersphere, compared to common kernels.

Below we derive the eigenfunctions of NTK for deep FC networks with and without bias. We note that [6, 12] derived the eigenfunctions of NTK for two-layer FC networks with no bias. We will show that the same eigenfunctions are obtained with deep, bias-free networks, and that additional eigenfunctions appear when bias is added. We begin with a definition.

Definition 1. A kernel \mathbf{k} is homogeneous of order α if $\mathbf{k}(\mathbf{x}, \mathbf{z}) = \|\mathbf{x}\|^\alpha \|\mathbf{z}\|^\alpha \mathbf{k}\left(\frac{\mathbf{x}^T \mathbf{z}}{\|\mathbf{x}\| \|\mathbf{z}\|}\right)$.

Theorem 4. (1) Bias-free $\mathbf{k}^{\text{FC}_0(\text{L})}$ is homogeneous of order 1. (2) With bias initialized at zero, let $\mathbf{k}^{\text{Bias}(\text{L})} = \mathbf{k}^{\text{FC}_\beta(\text{L})} - \mathbf{k}^{\text{FC}_0(\text{L})}$. Then, $\mathbf{k}^{\text{Bias}(\text{L})}$ is homogeneous of order 0.

The two kernels $\mathbf{k}^{\text{FC}_0(\text{L})}$ and $\mathbf{k}^{\text{FC}_\beta(\text{L})}$ (but not $\mathbf{k}^{\text{Bias}(\text{L})}$) are unbounded. Therefore, their Mercer's representation (1) exists under measures that decay sufficiently fast as $\|\mathbf{x}\| \rightarrow \infty$. Examples include the uniform distribution on the $\|\mathbf{x}\| \leq 1$ disk or the standard normal distribution. Such distributions have the virtue of being uniform on all concentric spheres. The following theorem determines the eigenfunctions for these kernels.

Theorem 5. Let $p(r)$ be a decaying density on $[0, \infty)$ such that $0 < \int_0^\infty p(r) r^2 dr < \infty$ and $\mathbf{x}, \mathbf{z} \in \mathbb{R}^d$.

1. Let $\mathbf{k}_0(\mathbf{x}, \mathbf{z})$ be homogeneous of order 1 such that $\mathbf{k}_0(\mathbf{x}, \mathbf{z}) = \|\mathbf{x}\| \|\mathbf{z}\| \hat{\mathbf{k}}_0\left(\frac{\mathbf{x}^T \mathbf{z}}{\|\mathbf{x}\| \|\mathbf{z}\|}\right)$. Then its eigenfunctions with respect to $p(\|\mathbf{x}\|)$ are given by $\Psi_{k,j} = a \|\mathbf{x}\| Y_{k,j}\left(\frac{\mathbf{x}}{\|\mathbf{x}\|}\right)$ where $Y_{k,j}$ are the spherical harmonics in \mathbb{S}^{d-1} and $a \in \mathbb{R}$.
2. Let $\mathbf{k}(\mathbf{x}, \mathbf{y}) = \mathbf{k}_0(\mathbf{x}, \mathbf{y}) + \mathbf{k}_1(\mathbf{x}, \mathbf{y})$ so that \mathbf{k}_0 as in 1 and \mathbf{k}_1 is homogeneous of order 0. Then the eigenfunctions of \mathbf{k} are of the form $\Psi_{k,j} = (a \|\mathbf{x}\| + b) Y_{k,j}\left(\frac{\mathbf{x}}{\|\mathbf{x}\|}\right)$.

The eigenfunctions of NTK in \mathbb{R}^d , therefore, are similar to those in \mathbb{S}^{d-1} ; they are the spherical harmonics scaled radially in the bias free case, or linearly with the norm when bias is used. With bias, $\mathbf{k}^{\text{FC}_\beta(\text{L})}$ has up to $2N(d, k)$ eigenfunctions for every frequency k .

In contrast to NTK, the Laplace kernel is shift invariant, and therefore its eigenfunctions are the Fourier transform. The two kernels hence cannot be compared merely by their eigenvalues. Figure 2 shows the eigenfunctions of NTK along with their correlation to the eigenfunctions of the Laplace kernel. While these differences are large, they seem to make only little difference in experiments, see Section 4 below. It is possible to produce a homogeneous version of the Laplace kernel as follows

$$\mathbf{k}^{\text{HLap}}(\mathbf{x}, \mathbf{y}) = \|\mathbf{x}\| \|\mathbf{y}\| \exp\left(-c \sqrt{1 - \frac{\mathbf{x}^T \mathbf{y}}{\|\mathbf{x}\| \|\mathbf{y}\|}}\right). \quad (4)$$

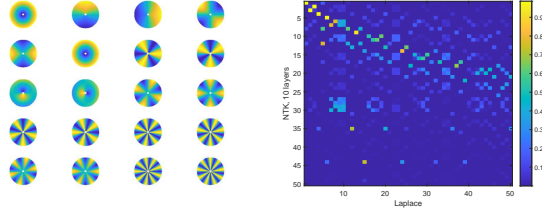


Figure 2: Left: plots of the eigenfunctions of NTK for a two layer FC network with bias on the unit disk, arranged in decreasing order of the eigenvalues. The radial shape of the eigenfunctions is evident. For two layers, the eigenvalues of $k^{\text{FC}_0(2)}$ are zero for odd $k \geq 3$, while those of $k^{\text{Bias}(2)}$ are zero for even $k \geq 2$. Therefore we see two “DC components” (top left and 2nd in 2nd row) and four $k = 1$ components (2nd and 3rd in 1st row and 1st and 2nd in third row). The rest of the frequencies are represented twice each. Right: Absolute correlation between the eigenfunctions of NTK and those of the Laplace kernel for data sampled uniformly on the unit disk. It can be seen that eigenfunctions of higher frequency for NTK correlate with eigenfunctions of higher frequency for the Laplace. However, relatively low order components for NTK contain higher frequency components of the Laplace.

Following Thm. 5 the eigenfunctions of this kernel are the scaled spherical harmonics and, following Thm. 2, its eigenvalues decay at the rate of k^{-d} , much like the NTK.

4 Experiments

We compare the performance of NTK with Laplace, Gaussian, and γ -exponential kernels on both small and large scale real datasets. Our goal is to demonstrate: a) Results with the Laplace kernel are quite similar to those obtained by NTK, and b) The γ -exponential kernel can achieve slightly better results than NTK. Experimental details are provided in the supplementary material.

4.1 UCI dataSet

We compare methods using the same set of 90 small scale UCI datasets (with less than 5000 data points) as in [4]. The results are provided in Table 1 for the exponential kernels and their homogeneous versions, denoted by the “H-” prefix, as well as for NTK. For completeness, we also cite the results for Random forest (RF), the top classifier identified in [23], and neural networks from [4].

We report the same metrics as used in [4]: Friedman Ranking, Average Accuracy, P90/P95, and PMA. A superior classifier is expected to have lower Friedman rank and higher P90, P95, and PMA. Friedman Ranking [21] reports the average ranking of a given classifier compared to other classifiers. P90/P95 denotes the fraction of datasets on which a classifier achieves more than 90/95% of the maximum achievable accuracy (i.e., maximum accuracy among all the classifiers [23]). PMA represents the percentage of maximum accuracy.

From Table 1, one can observe that the Laplace kernel results are the closest to NTK on all the metrics, and γ -exponential outperforms all the classifiers including NTK on all metrics. Moreover, the homogeneous versions slightly outperform the standard kernels. All these methods have hyperparameters that can be optimized. In [4], they search 105 hyperparameters for NTK. For a fair comparison, we search for the same number for the γ -exponential and fewer (70) for the Laplace kernels.

4.2 Large scale datasets

We leverage FALKON [41], an efficient approximate kernel method to conduct large scale regression and classification tasks following the setup of [41]. The results and datasets details are reported in Table 2. We searched for hyperparameters based on a small validation dataset for all the methods and used the standard train/test partition provided on the UCI repository. From Table 2, one can notice that NTK and Laplace perform similarly. For each dataset, either the γ -exponential or Gaussian kernels slightly outperforms these two kernels.

Classifier	F. Rank	Average Accuracy	P90	P95	PMA
H- γ -exp.	26.26	82.25% \pm 14.07%	92.22%	73.33%	96.07% \pm 4.83%
γ -exp.	32.98	81.80% \pm 14.21%	85.56%	73.33%	95.49% \pm 5.31%
H-Laplace	29.60	81.74% \pm 13.82%	88.89%	66.67%	95.53% \pm 4.84%
Laplace	33.28	81.12% \pm 14.16%	86.67%	65.56%	94.88% \pm 6.85%
H-Gaussian	32.66	81.46% \pm 14.83%	84.44%	67.77%	94.95% \pm 6.25%
Gaussian	35.76	81.03% \pm 15.09%	85.56%	72.22%	94.56% \pm 8.22%
NTK [4]	28.34	81.95% \pm 14.10%	88.89%	72.22%	95.72% \pm 5.17%
NN [4]	38.06	81.02% \pm 14.47%	85.56%	60.00%	94.55% \pm 5.89%
RF [4]	33.51	81.56% \pm 13.90%	85.56%	67.78%	95.25% \pm 5.30%

Table 1: Performance on the UCI dataset. Lower F. Rank and higher P90, P95, PMA are better numbers.

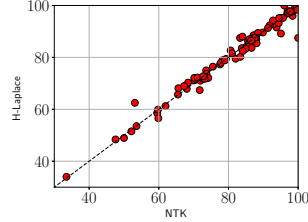


Figure 3: Performance comparisons between NTK and H-Laplace.

	MillionSongs [11]	SUSY [39]	HIGGS [39]
#Training Data	4.6×10^5	5×10^6	1.1×10^7
#Features	90	18	28
Problem Type	Regression	Classification	Classification
Performance Metric	MSE	AUC	AUC
H- γ -exp.	78.6417	87.686	82.281
H-Laplace	79.7941	87.670	81.995
NTK	79.9666	87.673	82.089
H-Gaussian	79.6255	87.689	81.967
Neural Network [39]	-	87.500	81.600
Deep Neural Network [39]	-	87.900*	88.500*

Table 2: Performance on the large scale datasets. We report MSE (lower is better) for the regression problem, and AUC (higher is better) for the classification problems.

4.3 Hierarchical convolutional kernels

Convolutional NTKs (CNTK) were shown to express the limit of convolutional neural networks when the number of channels tends to infinity, and recent empirical results showed that the two achieve similar accuracy on test data [2, 30]. CNTK is defined roughly by recursively applying NTK to image patches. For our final experiment we constructed alternative hierarchical kernels, in the spirit of [13, 32], by recursively applying exponential kernels in a manner similar to CNTK. The new kernel, denoted C-Exp, is applied first to pairs of 3×3 image patches, then to 3×3 patches of kernel values, and so forth. A detailed algorithm is provided in the supplementary material. We applied the kernel (using the homogeneous versions of the Laplace, Gaussian and γ -exponential kernels) to the Cifar-10 dataset and compared it to CNTK. Our experimental conditions and results for CNTK are identical to those of [2]. Consistent with our previous experiments, Table 3 shows that these kernels are on par with the CNTK with small advantage to the γ -exponential kernel. This demonstrates that the four kernels maintain similar performance even after repeated application.

Method	Accuracy (50k)	Accuracy(2k)
CNTK	66.4%	43.9%
C-Exp Laplace	65.2%	44.2%
C-Exp γ -exponential	67.0%	45.2%
C-Exp Gaussian	66.8%	45.0%

Table 3: Classification accuracy for the CIFAR-10 dataset for our C-Exp hierarchical kernels, compared to CNTK. The two columns show results with training on the full dataset and on the first 2000 examples.

5 Conclusions

Our paper has considered the relationship between NTK and the classic Laplace kernel. Our main result is to show that for data normalized on the unit hypersphere, these two kernels have the same RKHS. Experiments show that the two kernels perform almost identically on a wide range of real-world applications. Coupled with prior results that show that kernel methods using NTK mimic the behavior of FC neural networks, our results suggest that much insight about neural networks can be obtained from analysis of the well-known Laplace kernel, which has a simple closed form.

Neural networks do offer great flexibility not easily translated to kernel methods. They can naturally be applied to large data sets, and researchers have developed many techniques for training them, such as dropout and batch normalization, that improve performance but do not directly translate to

kernel methods. Furthermore, while we study feed-forward fully connected networks, analyzing more complex architectures, such as CNNs, GANs, autoencoders and recurrent networks remains a significant challenge for future work.

Acknowledgements

The authors thank the U.S.- Israel Binational Science Foundation, grant number 2018680, the National Science Foundation, grant no. IIS-1910132, the Quantifying Ensemble Diversity for Robust Machine Learning (QED for RML) program from DARPA and the Guaranteeing AI Robustness Against Deception (GARD) program from DARPA for their support of this project.

References

- [1] Zeyuan Allen-Zhu, Yuanzhi Li, and Zhao Song. A convergence theory for deep learning via overparameterization. In Kamalika Chaudhuri and Ruslan Salakhutdinov, editors, *Proceedings of the 36th International Conference on Machine Learning*, volume 97, pages 242–252, 2019.
- [2] Sanjeev Arora, Simon S Du, Wei Hu, Zhiyuan Li, Russ R Salakhutdinov, and Ruosong Wang. On exact computation with an infinitely wide neural net. In *Advances in Neural Information Processing Systems*, pages 8139–8148, 2019.
- [3] Sanjeev Arora, Simon S Du, Wei Hu, Zhiyuan Li, and Ruosong Wang. Fine-grained analysis of optimization and generalization for overparameterized two-layer neural networks. *arXiv preprint arXiv:1901.08584*, 2019.
- [4] Sanjeev Arora, Simon S Du, Zhiyuan Li, Ruslan Salakhutdinov, Ruosong Wang, and Dingli Yu. Harnessing the power of infinitely wide deep nets on small-data tasks. *arXiv preprint arXiv:1910.01663*, 2019.
- [5] Sanjeev Arora, Simon S. Du, Zhiyuan Li, Ruslan Salakhutdinov, Ruosong Wang, and Dingli Yu. Harnessing the power of infinitely wide deep nets on small-data tasks. In *International Conference on Learning Representations*, 2020.
- [6] Francis Bach. Breaking the curse of dimensionality with convex neural networks. *The Journal of Machine Learning Research*, 18(1):629–681, 2017.
- [7] Ronen Basri, Meirav Galun, Amnon Geifman, David Jacobs, Yoni Kasten, and Shira Kritchman. Frequency bias in neural networks for input of non-uniform density, 2020.
- [8] Ronen Basri, David Jacobs, Yoni Kasten, and Shira Kritchman. The convergence rate of neural networks for learned functions of different frequencies. In *Advances in Neural Information Processing Systems*, pages 4763–4772, 2019.
- [9] Mikhail Belkin, Daniel J Hsu, and Partha Mitra. Overfitting or perfect fitting? risk bounds for classification and regression rules that interpolate. In *Advances in neural information processing systems*, pages 2300–2311, 2018.
- [10] Mikhail Belkin, Siyuan Ma, and Soumik Mandal. To understand deep learning we need to understand kernel learning. *arXiv preprint arXiv:1802.01396*, 2018.
- [11] Thierry Bertin-Mahieux, Daniel PW Ellis, Brian Whitman, and Paul Lamere. The million song dataset. 2011.
- [12] Alberto Bietti and Julien Mairal. On the inductive bias of neural tangent kernels. In *Advances in Neural Information Processing Systems*, pages 12873–12884, 2019.
- [13] Liefeng Bo, Xiaofeng Ren, and Dieter Fox. Kernel descriptors for visual recognition. In J. D. Lafferty, C. K. I. Williams, J. Shawe-Taylor, R. S. Zemel, and A. Culotta, editors, *Advances in Neural Information Processing Systems 23*, pages 244–252. 2010.
- [14] Blake Bordelon, Abdulkadir Canatar, and Cengiz Pehlevan. Spectrum dependent learning curves in kernel regression and wide neural networks. *arXiv preprint arXiv:2002.02561*, 2020.
- [15] Yuan Cao, Zhiying Fang, Yue Wu, Ding-Xuan Zhou, and Quanquan Gu. Towards understanding the spectral bias of deep learning. *arXiv preprint arXiv:1912.01198*, 2019.
- [16] Olivier Chapelle. Training a support vector machine in the primal. *Neural computation*, 19(5):1155–1178, 2007.
- [17] Youngmin Cho and Lawrence K Saul. Kernel methods for deep learning. In *Advances in neural information processing systems*, pages 342–350, 2009.
- [18] Youngmin Cho and Lawrence K Saul. Analysis and extension of arc-cosine kernels for large margin classification. *arXiv preprint arXiv:1112.3712*, 2011.
- [19] Bo Dai, Bo Xie, Niao He, Yingyu Liang, Anant Raj, Maria-Florina F Balcan, and Le Song. Scalable kernel methods via doubly stochastic gradients. In *Advances in Neural Information Processing Systems*, pages 3041–3049, 2014.

- [20] Amit Daniely, Roy Frostig, and Yoram Singer. Toward deeper understanding of neural networks: The power of initialization and a dual view on expressivity. In *Advances In Neural Information Processing Systems*, pages 2253–2261, 2016.
- [21] Janez Demšar. Statistical comparisons of classifiers over multiple data sets. *Journal of Machine learning research*, 7(Jan):1–30, 2006.
- [22] Zhou Fan and Zhichao Wang. Spectra of the conjugate kernel and neural tangent kernel for linear-width neural networks. *arXiv preprint arXiv:2005.11879*, 2020.
- [23] Manuel Fernández-Delgado, Eva Cernadas, Senén Barro, and Dinani Amorim. Do we need hundreds of classifiers to solve real world classification problems? *The journal of machine learning research*, 15(1):3133–3181, 2014.
- [24] Marc G. Genton. Classes of kernels for machine learning: A statistics perspective. *Journal of Machine Learning Research*, 2:299–312, 2001.
- [25] Behrooz Ghorbani, Song Mei, Theodor Misiakiewicz, and Andrea Montanari. Linearized two-layers neural networks in high dimension. *arXiv preprint arXiv:1904.12191*, 2019.
- [26] Kaixuan Huang, Yuqing Wang, Molei Tao, and Tuo Zhao. Why do deep residual networks generalize better than deep feedforward networks?—a neural tangent kernel perspective. *arXiv preprint arXiv:2002.06262*, 2020.
- [27] Arthur Jacot, Franck Gabriel, and Clément Hongler. Neural tangent kernel: Convergence and generalization in neural networks. In *Advances in neural information processing systems*, pages 8571–8580, 2018.
- [28] Kurt Jetter, Joachim StÅkckler, and Joseph Ward. Error estimates for scattered data interpolation on spheres. *Mathematics of Computation*, 68(226):733–747, 1999.
- [29] George S Kimeldorf and Grace Wahba. A correspondence between bayesian estimation on stochastic processes and smoothing by splines. *The Annals of Mathematical Statistics*, 41(2):495–502, 1970.
- [30] Zhiyuan Li, Ruosong Wang, Dingli Yu, Simon S Du, Wei Hu, Ruslan Salakhutdinov, and Sanjeev Arora. Enhanced convolutional neural tangent kernels. *arXiv preprint arXiv:1911.00809*, 2019.
- [31] Tengyuan Liang and Alexander Rakhlin. Just interpolate: Kernel" ridgeless" regression can generalize. *arXiv preprint arXiv:1808.00387*, 2018.
- [32] Julien Mairal, Piotr Koniusz, Zaid Harchaoui, and Cordelia Schmid. Convolutional kernel networks. In Z. Ghahramani, M. Welling, C. Cortes, N. D. Lawrence, and K. Q. Weinberger, editors, *Advances in Neural Information Processing Systems 27*, pages 2627–2635. 2014.
- [33] Charles A Micchelli and Grace Wahba. Design problems for optimal surface interpolation. Technical report, WISCONSIN UNIV-MADISON DEPT OF STATISTICS, 1979.
- [34] Ha Quang Minh, Partha Niyogi, and Yuan Yao. Mercer’s theorem, feature maps, and smoothing. In *International Conference on Computational Learning Theory*, pages 154–168. Springer, 2006.
- [35] Francis J Narcowich, Xinping Sun, and Joseph D Ward. Approximation power of rbfs and their associated sbfs: a connection. *Advances in Computational Mathematics*, 27(1):107–124, 2007.
- [36] Francis J Narcowich and Joseph D Ward. Scattered data interpolation on spheres: error estimates and locally supported basis functions. *SIAM Journal on Mathematical Analysis*, 33(6):1393–1410, 2002.
- [37] Radford M Neal. *Bayesian learning for neural networks*, volume 118. Springer Science & Business Media, 2012.
- [38] Roman Novak, Lechao Xiao, Jaehoon Lee, Yasaman Bahri, Greg Yang, Jiri Hron, Daniel A Abolafia, Jeffrey Pennington, and Jascha Sohl-Dickstein. Bayesian deep convolutional networks with many channels are gaussian processes. *arXiv preprint arXiv:1810.05148*, 2018.
- [39] Peter Sadowski Pierre Baldi and Daniel Whiteson. Searching for exotic particles in high-energy physics with deep learning. *Nature communications*, 5, 2014.
- [40] Carl Edward Rasmussen and Christopher K. I. Williams. *Gaussian Processes for Machine Learning*. MIT Press, 2006.
- [41] Alessandro Rudi, Luigi Carratino, and Lorenzo Rosasco. Falkon: An optimal large scale kernel method. In *Advances in Neural Information Processing Systems*, pages 3888–3898, 2017.
- [42] Saburo Saitoh and Yoshihiro Sawano. *Theory of reproducing kernels and applications*. Springer, 2016.
- [43] Bernhard Scholkopf and Alexander J Smola. *Learning with kernels: support vector machines, regularization, optimization, and beyond*. MIT press, 2001.
- [44] Elias M Stein and Guido Weiss. *Introduction to Fourier analysis on Euclidean spaces (PMS-32)*, volume 32. Princeton university press, 2016.
- [45] George Neville Watson. *A treatise on the theory of Bessel functions*. Cambridge university press, 1966.
- [46] Christopher KI Williams. Computing with infinite networks. In *Advances in neural information processing systems*, pages 295–301, 1997.
- [47] Greg Yang and Hadi Salman. A fine-grained spectral perspective on neural networks. *arXiv preprint arXiv:1907.10599*, 2019.

A Formulas for NTK

We begin by providing the recursive definition of NTK for fully connected (FC) networks with bias initialized at zero. The formulation includes a parameter β that when set to zero the recursive formula coincides with the formula given in [2] for bias-free networks.

The network model We consider a L -hidden-layer fully-connected neural network (in total $L + 1$ layers) with bias. Let $\mathbf{x} \in \mathbb{R}^d$ (and denote $d_0 = d$), we assume each layer $l \in [L]$ of hidden units includes d_l units. The network model is expressed as

$$\begin{aligned} \mathbf{g}^{(0)}(\mathbf{x}) &= \mathbf{x} \\ \mathbf{f}^{(l)}(\mathbf{x}) &= W^{(l)} \mathbf{g}^{(l-1)}(\mathbf{x}) + \beta \mathbf{b}^{(l)} \in \mathbb{R}^{d_l}, \quad l = 1, \dots, L \\ \mathbf{g}^{(l)}(\mathbf{x}) &= \sqrt{\frac{c_\sigma}{d_l}} \sigma \left(\mathbf{f}^{(l)}(\mathbf{x}) \right) \in \mathbb{R}^{d_l}, \quad l = 1, \dots, L \\ f(\theta, \mathbf{x}) &= f^{(L+1)}(\mathbf{x}) = W^{(L+1)} \cdot \mathbf{g}^{(L)}(\mathbf{x}) + \beta b^{(L+1)} \end{aligned}$$

The network parameters θ include $W^{(L+1)}, W^{(L)}, \dots, W^{(1)}$, where $W^{(l)} \in \mathbb{R}^{d_l \times d_{l-1}}$, $\mathbf{b}^{(l)} \in \mathbb{R}^{d_l \times 1}$, $W^{(L+1)} \in \mathbb{R}^{1 \times d_L}$, $b^{(L+1)} \in \mathbb{R}$, σ is the activation function and $c_\sigma = 1 / (\mathbb{E}_{z \sim \mathcal{N}(0,1)}[\sigma(z)^2])$. The network parameters are initialized with $\mathcal{N}(0, I)$, except for the biases $\{\mathbf{b}^{(1)}, \dots, \mathbf{b}^{(L)}, b^{(L+1)}\}$, which are initialized with zero.

The recursive formula for NTK The recursive formula in [27] assumes the bias is initialized with a normal distribution. Here we assume the bias is initialized at zero, yielding a slightly different formulation, which can be readily derived from [27]'s formulation.

Given $\mathbf{x}, \mathbf{z} \in \mathbb{R}^d$, we denote the NTK for this fully connected network with bias by $\mathbf{k}^{\text{FC}_\beta(L+1)}(\mathbf{x}, \mathbf{z}) := \Theta^{(L)}(\mathbf{x}, \mathbf{z})$. The kernel $\Theta^{(L)}(\mathbf{x}, \mathbf{z})$ is defined using the following recursive definition. Let $h \in [L]$ then

$$\Theta^{(h)}(\mathbf{x}, \mathbf{z}) = \Theta^{(h-1)}(\mathbf{x}, \mathbf{z}) \dot{\Sigma}^{(h)}(\mathbf{x}, \mathbf{z}) + \Sigma^{(h)}(\mathbf{x}, \mathbf{z}) + \beta^2, \quad (5)$$

where

$$\begin{aligned} \Sigma^{(0)}(\mathbf{x}, \mathbf{z}) &= \mathbf{x}^T \mathbf{z} \\ \Theta^{(0)}(\mathbf{x}, \mathbf{z}) &= \Sigma^{(0)}(\mathbf{x}, \mathbf{z}) + \beta^2. \end{aligned}$$

Now, let

$$\lambda^{(h-1)}(\mathbf{x}, \mathbf{z}) = \frac{\Sigma^{(h-1)}(\mathbf{x}, \mathbf{z})}{\sqrt{\Sigma^{(h-1)}(\mathbf{x}, \mathbf{x}) \Sigma^{(h-1)}(\mathbf{z}, \mathbf{z})}}. \quad (6)$$

$|\lambda^{(h-1)}| \leq 1$ and we define

$$\Sigma^{(h)}(\mathbf{x}, \mathbf{z}) = c_\sigma \frac{\lambda^{(h-1)}(\pi - \arccos(\lambda^{(h-1)})) + \sqrt{1 - (\lambda^{(h-1)})^2}}{2\pi} \sqrt{\Sigma^{(h-1)}(\mathbf{x}, \mathbf{x}) \Sigma^{(h-1)}(\mathbf{z}, \mathbf{z})} \quad (7)$$

$$\dot{\Sigma}^{(h)}(\mathbf{x}, \mathbf{z}) = c_\sigma \frac{\pi - \arccos(\lambda^{(h-1)})}{2\pi}, \quad (8)$$

where for the ReLU activation function $c_\sigma = 2$. The parameter β allows us to consider a fully-connected network either with ($\beta > 0$) or without bias ($\beta = 0$). In the case $\beta = 0$, the recursive formulation is the same as existing derivations, e.g. [27]. Finally, the normalized NTK of a FC network with $L + 1$ layers, without bias, is given by $\frac{1}{L+1} \mathbf{k}^{\text{FC}_0(L+1)}(\mathbf{x}_i, \mathbf{x}_j)$.

NTK for a two-layer FC network on \mathbb{S}^{d-1} Using the recursive formulation above, NTK for a two-layer FC network with bias initialized at 0, for points on the hypersphere \mathbb{S}^{d-1} is given by

$$\mathbf{k}^{\text{FC}_\beta(2)}(\mathbf{x}, \mathbf{z}) = \mathbf{k}^{\text{FC}_\beta(2)}(u) = \frac{1}{\pi} \left((2u + \beta^2)(\pi - \arccos(u)) + \sqrt{1 - u^2} \right) + \beta^2, \quad (9)$$

where $u = \mathbf{x}^T \mathbf{z}$, with $\mathbf{x}, \mathbf{z} \in \mathbb{S}^{d-1}$. This is derived as follows

$$\begin{aligned}
\mathbf{k}^{\text{FC}_\beta(2)}(\mathbf{x}, \mathbf{z}) &= \Theta^{(1)}(\mathbf{x}, \mathbf{z}) \\
&= \Theta^{(0)}(\mathbf{x}, \mathbf{z}) \dot{\Sigma}^{(1)}(\mathbf{x}, \mathbf{z}) + \Sigma^{(1)}(\mathbf{x}, \mathbf{z}) + \beta^2 \\
&= (u + \beta^2) \frac{\pi - \arccos(u)}{\pi} + \frac{u(\pi - \arccos(u)) + \sqrt{1 - u^2}}{\pi} + \beta^2 \\
&= \frac{1}{\pi} \left((2u + \beta^2)(\pi - \arccos(u)) + \sqrt{1 - u^2} \right) + \beta^2
\end{aligned}$$

B NTK on \mathbb{S}^{d-1}

This section provides a characterization of NTK on the hypersphere \mathbb{S}^{d-1} under the uniform measure. The recursive formulas of the kernels are given in Appendix A.

Lemma 2. *Let $\mathbf{k}^{\text{FC}_\beta(L)}(\mathbf{x}, \mathbf{z})$, $\mathbf{x}, \mathbf{z} \in \mathbb{S}^{d-1}$, denote the NTK kernels for FC networks with $L \geq 2$ layers, possibly with bias initialized with zero. This kernel is zonal, i.e., $\mathbf{k}^{\text{FC}_\beta(L)}(\mathbf{x}, \mathbf{z}) = \mathbf{k}^{\text{FC}_\beta(L)}(\mathbf{x}^T \mathbf{z})$.*

Proof. See Appendix D. □

To prove the next theorem, we recall several results on the the arithmetics of RKHS, following [20, 42].

B.1 RKHS for sums and products of kernels.

Let $\mathbf{k}_1, \mathbf{k}_2 : \mathcal{X} \times \mathcal{X} \rightarrow \mathbb{R}$ be kernels with RKHS $\mathcal{H}_{\mathbf{k}_1}$ and $\mathcal{H}_{\mathbf{k}_2}$, respectively. Then,

1. **Aronszajn's kernel sum theorem.** The RKHS for $\mathbf{k} = \mathbf{k}_1 + \mathbf{k}_2$ is given by $\mathcal{H}_{\mathbf{k}_1 + \mathbf{k}_2} = \{f_1 + f_2 \mid f_1 \in \mathcal{H}_{\mathbf{k}_1}, f_2 \in \mathcal{H}_{\mathbf{k}_2}\}$
2. This yields the **kernel sum inclusion**. $\mathcal{H}_{\mathbf{k}_1}, \mathcal{H}_{\mathbf{k}_2} \subseteq \mathcal{H}_{\mathbf{k}_1 + \mathbf{k}_2}$
3. **Norm addition inequality.** $\|f_1 + f_2\|_{\mathcal{H}_{\mathbf{k}_1 + \mathbf{k}_2}} \leq \|f_1\|_{\mathcal{H}_{\mathbf{k}_1}} + \|f_2\|_{\mathcal{H}_{\mathbf{k}_2}}$
4. **Norm product inequality.** $\|f_1 \cdot f_2\|_{\mathcal{H}_{\mathbf{k}_1 \cdot \mathbf{k}_2}} \leq \|f_1\|_{\mathcal{H}_{\mathbf{k}_1}} \cdot \|f_2\|_{\mathcal{H}_{\mathbf{k}_2}}$
5. **Aronszajn's inclusion theorem.** $\mathcal{H}_{\mathbf{k}_1} \subseteq \mathcal{H}_{\mathbf{k}_2}$ if and only if $\exists s > 0$, such that $\mathbf{k}_1 \ll s^2 \mathbf{k}_2$, where the latter notation means that $s^2 \mathbf{k}_2 - \mathbf{k}_1$ is a positive definite kernel over \mathcal{X} .

B.2 The decay rate of the eigenvalues of NTK

Theorem 6. *Let $\mathbf{x}, \mathbf{z} \in \mathbb{S}^{d-1}$. With bias initialized at zero and $\beta > 0$:*

1. $\mathbf{k}^{\text{FC}_\beta(L)}$ can be decomposed according to

$$\mathbf{k}^{\text{FC}_\beta(L)}(\mathbf{x}, \mathbf{z}) = \sum_{k=0}^{\infty} \lambda_k \sum_{j=1}^{N(d,k)} Y_{k,j}(\mathbf{x}) Y_{k,j}(\mathbf{z}), \quad (10)$$

with $\lambda_k > 0$ for all $k \geq 0$ and into $Y_{k,j}$ are the spherical harmonics of \mathbb{S}^{d-1} , and

2. $\exists k_0$ and constants $C_1, C_2, C_3 > 0$ that depend on the dimension d such that $\forall k > k_0$
 - (a) $C_1 k^{-d} \leq \lambda_k \leq C_2 k^{-d}$ if $L = 2$, and
 - (b) $C_3 k^{-d} \leq \lambda_k$ if $L \geq 3$.

We split the theorem into the next two lemmas. The first lemma handles NTK of two-layer FC networks with bias, and the second lemma handles NTK for deep networks.

Lemma 3. Let $\mathbf{x}, \mathbf{z} \in \mathbb{S}^{d-1}$ and $\mathbf{k}^{\text{FC}_\beta(2)}(\mathbf{x}^T \mathbf{z})$ as defined in (9) with $\beta > 0$. Then, $\mathbf{k}^{\text{FC}_\beta(2)}$ decomposes according to (10) where $\lambda_k > 0$ for all $k \geq 0$ and $\exists k_0$ such that $\forall k \geq k_0$

$$C_1 k^{-d} \leq \lambda_k \leq C_2 k^{-d},$$

where $C_1, C_2 > 0$ are constants that depend on the dimension d .

Proof. To prove the lemma we leverage the results of [6, 12]. First, under the assumption of the uniform measure on \mathbb{S}^{d-1} , we can apply Mercer decomposition to $\mathbf{k}^{\text{FC}_\beta(2)}(\mathbf{x}, \mathbf{z})$, where the eigenfunctions are the spherical harmonics. This is due to the observation that $\mathbf{k}^{\text{FC}_\beta(2)}(\mathbf{x}, \mathbf{z})$ is positive and zonal in \mathbb{S}^{d-1} . It is zonal by Lemma 2 and positive, since $\mathbf{k}^{\text{FC}_\beta(2)}$ can be decomposed as

$$\begin{aligned} \mathbf{k}^{\text{FC}_\beta(2)}(u) &= \frac{1}{\pi} \left((2u + \beta^2)(\pi - \arccos(u)) + \sqrt{1 - u^2} \right) + \beta^2 \\ &= \frac{1}{\pi} \left(2u(\pi - \arccos(u)) + \sqrt{1 - u^2} \right) + \frac{1}{\pi} \beta^2 (\pi - \arccos(u)) + \beta^2 \\ &:= \kappa(\mathbf{x}^T \mathbf{z}) + \beta^2 \kappa_0(\mathbf{x}^T \mathbf{z}) + \beta^2, \end{aligned}$$

where $\kappa(\mathbf{x}^T \mathbf{z})$ is the NTK for a bias-free, two-layer network introduced in [12] and $\kappa_0(\mathbf{x}^T \mathbf{z})$ is known to be the zero-order arc-cosine kernel [18]. By kernel arithmetic, this yields another kernel and this means that $\mathbf{k}^{\text{FC}_\beta(2)}$ is a positive kernel.

Furthermore, according to Proposition 5 in [12]

$$\kappa(\mathbf{x}^T \mathbf{z}) = \sum_{k=0}^{\infty} \mu_k \sum_{j=1}^{N(d,k)} Y_{k,j}(\mathbf{x}) Y_{k,j}(\mathbf{z}),$$

where $Y_{k,j}, j = 1, \dots, N(d, k)$ are spherical harmonics of degree k , and the eigenvalues μ_k satisfy $\mu_0, \mu_1 > 0, \mu_k = 0$ if $k = 2j + 1$ with $j \geq 1$ and otherwise, $\mu_k > 0$ and $\mu_k \sim C(d)k^{-d}$ as $k \rightarrow \infty$, with $C(d)$ a constant depending only on d . Next, following Lemma 17 in [12] the eigenvalues of $\kappa_0(\mathbf{x}^T \mathbf{z})$, denoted η_k satisfy $\eta_0, \eta_1 > 0, \eta_k > 0$ if $k = 2j + 1$, with $j \geq 1$ and behave asymptotically as $C_0(d)k^{-d}$. Consequently, $\mathbf{k}^{\text{FC}_\beta(2)} = \kappa + \beta^2 \kappa_0 + \beta^2$, and since both κ and κ_0 have the spherical harmonics as their eigenfunctions, their eigenvalues are given by $\lambda_k = \mu_k + \beta^2 \eta_k > 0$ for $k > 0$ and $\lambda_0 = \mu_0 + \beta^2 \eta_0 + \beta^2 > 0$, and asymptotically $\lambda_k \sim \tilde{C}(d)k^{-d}$, where $\tilde{C}(d) = C(d) + \beta^2 C_0(d)$.

To conclude, this implies that $\exists k_0, C_1(d) > 0$ and $C_2(d) > 0$, such that for all $k \geq k_0$ it holds that

$$C_1 k^{-d} \leq \lambda_k \leq C_2 k^{-d}$$

and also, unless $\beta = 0$, for all $k \geq 0$

$$\lambda_k > 0.$$

□

Next, we prove the second part of Theorem 6 that relates to deep FC networks with bias, $\mathbf{k}^{\text{FC}_\beta(\text{L})}$, i.e. we prove the following lemma.

Lemma 4. Let $\mathbf{x}, \mathbf{z} \in \mathbb{S}^{d-1}$ and $\mathbf{k}^{\text{FC}_\beta(\text{L})}(\mathbf{x}^T \mathbf{z})$ as defined in Appendix A. Then

1. $\mathbf{k}^{\text{FC}_\beta(\text{L})}$ decomposes according to (10) with $\lambda_k > 0$ for all $k \geq 0$
2. $\exists k_0$ such that $\forall k > k_0$ it holds that $C_3 k^{-d} \leq \lambda_k$ in which $C_3 > 0$ depends on the dimension d
3. $\mathcal{H}^{\text{FC}_\beta(\text{L}-1)} \subseteq \mathcal{H}^{\text{FC}_\beta(\text{L})}$

Proof. Following Lemma 2, it holds that $\mathbf{k}^{\text{FC}_\beta(\text{L})}$ is zonal, and therefore can be decomposed according to (10). In order to prove the lemma we look at the recursive formulation of the NTK kernel, i.e.,

$$\mathbf{k}^{\text{FC}_\beta(\text{L}+1)} = \mathbf{k}^{\text{FC}_\beta(\text{L})} \dot{\Sigma}^{(\text{L})} + \Sigma^{(\text{L})} + \beta^2. \quad (11)$$

Now, following Lemma 17 in [12] all of the eigenvalues of $\dot{\Sigma}^{(\text{L})}$ are positive, including $\lambda_0 > 0$. This implies that the constant function $g(\mathbf{x}) \equiv 1 \in \mathcal{H}_{\dot{\Sigma}^{(\text{L})}}$.

Now, we use the norm multiplicity inequality in Sec. B.1 and show that $\mathcal{H}_{\mathbf{k}^{\text{FC}_\beta(1)}} \subseteq \mathcal{H}_{\mathbf{k}^{\text{FC}_\beta(1)} \cdot \dot{\Sigma}(1)}$. Let $f \in \mathcal{H}_{\mathbf{k}^{\text{FC}_\beta(1)}}$, i.e., $\|f\|_{\mathcal{H}_{\mathbf{k}^{\text{FC}_\beta(1)}}} < \infty$. We showed that $1 \in \mathcal{H}_{\dot{\Sigma}(1)}$. Therefore, $\|f \cdot 1\|_{\mathcal{H}_{\mathbf{k}^{\text{FC}_\beta(1)} \cdot \dot{\Sigma}(1)}} \leq \|f\|_{\mathcal{H}_{\mathbf{k}^{\text{FC}_\beta(1)}}} \|1\|_{\mathcal{H}_{\dot{\Sigma}(1)}} < \infty$, implying that $f \in \mathcal{H}_{\mathbf{k}^{\text{FC}_\beta(1)} \cdot \dot{\Sigma}(1)}$.

Finally, according to the kernel sum inclusion in Sec. B.1, relying on the recursive formulation (11) we have $\mathcal{H}_{\mathbf{k}^{\text{FC}_\beta(1)}} \subseteq \mathcal{H}_{\mathbf{k}^{\text{FC}_\beta(1)} \cdot \dot{\Sigma}(1)} \subseteq \mathcal{H}_{\mathbf{k}^{\text{FC}_\beta(1+1)}}$. Therefore,

$$\mathcal{H}^{\text{FC}_\beta(2)} \subseteq \dots \subseteq \mathcal{H}^{\text{FC}_\beta(L-1)} \subseteq \mathcal{H}^{\text{FC}_\beta(L)}. \quad (12)$$

This completes the proof, by using Aronszajn's inclusion theorem as follows. Since $H^{k^{\text{FC}(2)}} \subseteq H^{k^{\text{FC}(L)}}$, then by Aronszajn's inclusion theorem $\exists s > 0$ such that $\mathbf{k}^{\text{FC}_\beta(2)} \ll s^2 \mathbf{k}^{\text{FC}_\beta(L)}$. Since the kernels are zonal on the sphere (with uniform distribution of the data) their corresponding RKHS share the same eigenfunctions, namely the spherical harmonics.

Therefore, for all $k \geq 0$ it holds

$$s^2 \lambda_k^{\mathbf{k}^{\text{FC}_\beta(L)}} \geq \lambda_k^{\mathbf{k}^{\text{FC}_\beta(2)}} > 0$$

and for $k \rightarrow \infty$ it holds that

$$s^2 \lambda_k^{\mathbf{k}^{\text{FC}_\beta(L)}} \geq \lambda_k^{\mathbf{k}^{\text{FC}_\beta(2)}} \geq \frac{C_1}{k^d}$$

completing the proof. □

C Laplace Kernel in \mathbb{S}^{d-1}

The Laplace kernel $\mathbf{k}(\mathbf{x}, \mathbf{y}) = e^{-c\|\mathbf{x}-\mathbf{y}\|}$ restricted to the sphere \mathbb{S}^{d-1} is defined as

$$K(\mathbf{x}, \mathbf{y}) = \mathbf{k}(\mathbf{x}^T \mathbf{y}) = e^{-c\sqrt{1-\mathbf{x}^T \mathbf{y}}} \quad (13)$$

where $c > 0$ is a tuning parameter. We next prove an asymptotic bound on its eigenvalues.

Theorem 7. *Let $\mathbf{x}, \mathbf{y} \in \mathbb{S}^{d-1}$ and $\mathbf{k}(\mathbf{x}^T \mathbf{y}) = e^{-c\sqrt{1-\mathbf{x}^T \mathbf{y}}}$ be the Laplace kernel, restricted to \mathbb{S}^{d-1} . Then \mathbf{k} can be decomposed as in (10) with the eigenvalues λ_k satisfying $\lambda_k > 0$ for all $k \geq 0$ and $\exists k_0$ such that $\forall k > k_0$ it holds that:*

$$B_1 k^{-d} \leq \lambda_k \leq B_2 k^{-d}$$

where $B_1, B_2 > 0$ are constants that depend on the dimension d and the parameter c .

Our proof relies on several supporting lemmas.

Lemma 5. ([44] Thm 1.14 page 6) *For all $\alpha > 0$ it holds that*

$$\int_{\mathbb{R}^d} e^{-2\pi\|\mathbf{x}\|^\alpha} e^{-2\pi i \mathbf{t} \cdot \mathbf{x}} d\mathbf{x} = c_d \frac{\alpha}{(\alpha^2 + \|\mathbf{t}\|^2)^{(d+1)/2}}, \quad (14)$$

where $c_d = \Gamma(\frac{d+1}{2})/(\pi^{(d+1)/2})$

Lemma 6. *Let $f(\mathbf{x}) = e^{-c\|\mathbf{x}\|}$ with $\mathbf{x} \in \mathbb{R}^d$. Then, its Fourier transform $\Phi(\mathbf{w})$ with $\mathbf{w} \in \mathbb{R}^d$ is $\Phi(\mathbf{w}) = \Phi(\|\mathbf{w}\|) = C(1 + \|\mathbf{w}\|^2/c^2)^{-(d+1)/2}$ for some constant $C > 0$.*

Proof. To calculate the Fourier transform we need to calculate the following integral

$$\Phi(\mathbf{w}) = \frac{1}{(2\pi)^d} \int_{\mathbb{R}^d} e^{-c\|\mathbf{x}\|} e^{-i\mathbf{x} \cdot \mathbf{w}} d\mathbf{x}.$$

According to the Lemma 5, plugging $\alpha = \frac{c}{2\pi}$ and $\mathbf{t} = \frac{\mathbf{w}}{2\pi}$ into (14) yields

$$\Phi(\mathbf{w}) = c_d \frac{c}{(c^2 + \|\mathbf{w}\|^2)^{(d+1)/2}} = \frac{c_d}{c^{(d+1)}} \frac{1}{(1 + \frac{\|\mathbf{w}\|^2}{c^2})^{(d+1)/2}} = C \left(1 + \frac{\|\mathbf{w}\|^2}{c^2}\right)^{-(d+1)/2}$$

with $C = \frac{c_d}{c^{(d+1)}} > 0$. □

Lemma 7. ([36] Thm. 4.1) Let $f(\mathbf{x})$ be defined as $f(\|\mathbf{x}\|)$ for all $\mathbf{x} \in \mathbb{R}^d$, and let $\Phi(\mathbf{w}) = \Phi(\|\mathbf{w}\|)$ denote its Fourier Transform in \mathbb{R}^d . Then, its corresponding kernel on \mathbb{S}^{d-1} is defined as the restriction $\mathbf{k}(\mathbf{x}^T \mathbf{y}) = f(\|\mathbf{x} - \mathbf{y}\|)$ with $\mathbf{x}, \mathbf{y} \in \mathbb{S}^{d-1}$. By Mercer's Theorem the spherical harmonic expansion of $\mathbf{k}(\mathbf{x}^T \mathbf{y})$ is of the form

$$\mathbf{k}(\mathbf{x}^T \mathbf{y}) = \sum_{k=0}^{\infty} \lambda_k \sum_{j=1}^{N(d,k)} Y_{k,j}(\mathbf{x}) Y_{k,j}(\mathbf{y}).$$

Then, the eigenvalues in the spherical harmonic expansion λ_k are related to the Fourier coefficients of f , $\Phi(t)$, as follows

$$\lambda_k = \int_0^{\infty} t \Phi(t) J_{k+\frac{d-2}{2}}^2(t) dt, \quad (15)$$

where $J_v(t)$ is the usual Bessel function of the first kind of order v .

Having, these supporting Lemmas, we can now prove **Theorem 7**.

Proof. First, $\mathbf{k}(\cdot, \cdot)$ is a positive zonal kernel and hence can be written as

$$\mathbf{k}(\mathbf{x}^T \mathbf{y}) = \sum_{k=0}^{\infty} \lambda_k \sum_{j=1}^{N(d,k)} Y_{k,j}(\mathbf{x}) Y_{k,j}(\mathbf{y}).$$

Next, to derive the bounds we plug the Fourier coefficients, $\Phi(\omega)$, computed in Lemma 6, into the expression for the harmonic coefficients, λ_k (15), obtaining

$$\lambda_k = C \int_0^{\infty} \frac{t}{\left(1 + \frac{t^2}{c^2}\right)^{\frac{d+1}{2}}} J_{k+\frac{d-2}{2}}^2(t) dt.$$

Applying a change of variables $t = cx$ we get

$$\lambda_k = c^2 C \int_0^{\infty} \frac{x}{(1+x^2)^{\frac{d+1}{2}}} J_{k+\frac{d-2}{2}}^2(cx) dx. \quad (16)$$

We next bound this integral from both above and below. To get an upper bound we observe that for $x \in [0, \infty)$ $x^2 < 1 + x^2$, implying that $x(1+x^2)^{-(d+1)/2} < x^{-d}$, and consequently

$$\lambda_k < c^2 C \int_0^{\infty} x^{-d} J_{k+\frac{d-2}{2}}^2(cx) dx := c^2 C A(k, d, c).$$

The above integral $A(k, d, c)$ was computed in [45] (Sec. 13.41 page 402 with $a := c$, $\lambda := d$, and $\mu = \nu := k + (d-2)/2$) which gives

$$A(k, d, c) = \int_0^{\infty} x^{-d} J_{k+\frac{d-2}{2}}^2(cx) dx = \frac{\left(\frac{c}{2}\right)^{d-1} \Gamma(d) \Gamma(k - \frac{1}{2})}{2\Gamma^2(\frac{d+1}{2}) \Gamma(k + d - \frac{1}{2})}. \quad (17)$$

Using Stirling's formula $\Gamma(x) = \sqrt{2\pi} x^{x-1/2} e^{-x} (1 + O(x^{-1}))$ as $x \rightarrow \infty$. Consequently, for sufficiently large $k \gg d$

$$\begin{aligned} \lambda_k &< c^2 C A(k, d, c) = c^2 C \frac{\left(\frac{c}{2}\right)^{d-1} \Gamma(d) \Gamma(k - \frac{1}{2})}{2\Gamma^2(\frac{d+1}{2}) \Gamma(k + d - \frac{1}{2})} \\ &\sim c^2 C \frac{\left(\frac{c}{2}\right)^{d-1} \Gamma(d)}{2\Gamma^2(\frac{d+1}{2})} \cdot \frac{(k - \frac{1}{2})^{k-1} e^{-k+\frac{1}{2}}}{(k + d - \frac{1}{2})^{k+d-1} e^{-k-d+\frac{1}{2}}} (1 + O(k^{-1})) \\ &= B_2 k^{-d}, \end{aligned} \quad (18)$$

where B_2 depends on c , C and the dimension d .

We use again the relation (16) to derive a lower bound for λ_k . First, note that since $t, 1 + t^2, J_v^2(t)$ are all non-negative for $t \in [0, \infty)$ and therefore

$$\begin{aligned}\lambda_k &\geq c^2 C \int_1^\infty \frac{x}{(1+x^2)^{\frac{d+1}{2}}} J_{k+\frac{d-2}{2}}^2(cx) dx \geq c^2 C \int_1^\infty \frac{1}{2^{\frac{d+1}{2}} x^d} J_{k+\frac{d-2}{2}}^2(cx) dx \\ &= \frac{Cc^2}{2^{\frac{d+1}{2}}} \left(\int_0^\infty x^{-d} J_{k+\frac{d-2}{2}}^2(cx) dx - \int_0^1 x^{-d} J_{k+\frac{d-2}{2}}^2(cx) dx \right) \\ &= \frac{Cc^2}{2^{\frac{d+1}{2}}} \int_0^\infty x^{-d} J_{k+\frac{d-2}{2}}^2(cx) dx \left(1 - \frac{\int_0^1 x^{-d} J_{k+\frac{d-2}{2}}^2(cx) dx}{\int_0^\infty x^{-d} J_{k+\frac{d-2}{2}}^2(cx) dx} \right) \\ &= \frac{Cc^2}{2^{\frac{d+1}{2}}} A(k, d, c) \left(1 - \frac{B(k, d, c)}{A(k, d, c)} \right),\end{aligned}$$

where $B(k, d, c) := \int_0^1 x^{-d} J_{k+\frac{d-2}{2}}^2(cx) dx$. The first integral, $A(k, d, c)$, was shown in (18) to converge asymptotically to $B_2 k^{-d}$. To bound the second integral, $B(k, d, c)$, we use an inequality from [45] (Section 3.31, page 49), which states that for $v, t \in \mathbb{R}, v > -\frac{1}{2}$,

$$|J_v(t)| \leq \frac{2^{-v} t^v}{\Gamma(v+1)}.$$

This gives an upper bound for $B(k, d, c)$

$$B(k, d, c) = \int_0^1 x^{-d} J_{k+\frac{d-2}{2}}^2(cx) dx \leq \int_0^1 x^{-d} \frac{2^{-2(k+\frac{d-2}{2})} (cx)^{2(k+\frac{d-2}{2})}}{\Gamma^2(k+\frac{d}{2})} dx \leq \frac{(\frac{c}{2})^{2(k+\frac{d-2}{2})}}{\Gamma^2(k+\frac{d}{2})}.$$

Applying Stirling's formula we obtain $B(k, d, c) \leq O\left(\frac{(\frac{ce}{2})^{2(k+\frac{d}{2})} (k+d)}{(k+\frac{d}{2})^{2(k+\frac{d}{2})}}\right)$, which implies that as k grows, $\frac{B(k, d, c)}{A(k, d, c)} \rightarrow 0$. Therefore, asymptotically for large k

$$\lambda_k \geq \frac{Cc^2}{2^{\frac{d+1}{2}}} A(k, d, c) \left(1 - \frac{B(k, d, c)}{A(k, d, c)} \right) \geq \frac{Cc^2}{2^{\frac{d+1}{2}}} A(k, d, c),$$

from which we conclude that $\lambda_k > B_1 k^{-d}$, where the constant B_1 depends on c, C , and d . We have therefore shown that there exists k_0 such that $\forall k > k_0$

$$B_1 k^{-d} \leq \lambda_k \leq B_2 k^{-d}.$$

Finally, to show that $\lambda_k > 0$ for all $k \geq 0$ we use again (15) in Lemma 7 which states that

$$\lambda_k = \int_0^\infty t \Phi(t) J_{k+\frac{d-2}{2}}^2(t) dt.$$

Note that in the interval $(0, \infty)$ it holds that $t > 0$ and $\Phi(t) > 0$ due to Lemma 6. Therefore $\lambda_k = 0$ implies that $J_{k+\frac{d-2}{2}}^2(t)$ is identically 0 on $(0, \infty)$, contradicting the properties of the Bessel function of the first kind. Hence, $\lambda_k > 0$ for all k . \square

C.1 Proof of main theorem

Theorem 8. Let \mathcal{H}^{Lap} denote the RKHS for the Laplace kernel restricted to \mathbb{S}^{d-1} , and let $\mathcal{H}^{\text{FC}_\beta(\text{L})}$ denote the NTK corresponding to a FC network with L layers with bias, restricted to \mathbb{S}^{d-1} , then $\mathcal{H}^{\text{Lap}} = \mathcal{H}^{\text{FC}_\beta(2)} \subseteq \mathcal{H}^{\text{FC}_\beta(\text{L})}$.

Proof. Let $\lambda_k^{\text{Lap}}, \lambda_k^{\text{FC}_\beta(2)}$, and $\lambda_k^{\text{FC}_\beta(\text{L})}$ denote the eigenvalues of the three kernel, $\mathbf{k}^{\text{Lap}}, \mathbf{k}^{\text{FC}_\beta(2)}$, and $\mathbf{k}^{\text{FC}_\beta(\text{L})}$ in their Mercer's decomposition, i.e.,

$$\mathbf{k}(\mathbf{x}^T \mathbf{z}) = \sum_{k=0}^{\infty} \lambda_k \sum_{j=1}^{N(d,k)} Y_{k,j}(\mathbf{x}) Y_{k,j}(\mathbf{z}).$$

Denote by k_0 the smallest k for which Theorems 6 and 7 hold simultaneously. We first show that $\mathcal{H}^{\text{Lap}} \subseteq \mathcal{H}^{\text{FC}_\beta(2)}$. Let $f(\mathbf{x}) \in \mathcal{H}^{\text{Lap}}$, and let $f(\mathbf{x}) = \sum_{k=0}^{\infty} \sum_{j=0}^{N(d,k)} \alpha_{k,j} Y_{k,j}(\mathbf{x})$ denote its spherical harmonic decomposition. Then $\|f\|_{\mathcal{H}^{\text{Lap}}} < \infty$ implies, due to Theorem 7, that

$$\sum_{k=k_0}^{\infty} \sum_{j=0}^{N(d,k)} \frac{1}{B_2} k^d \alpha_{k,j}^2 \leq \sum_{k=k_0}^{\infty} \sum_{j=0}^{N(d,k)} \frac{\alpha_{k,j}^2}{\lambda_k^{\text{Lap}}} < \infty.$$

Combining this with Theorem 6, and recalling that $\lambda_k^{\text{FC}_\beta(2)} > 0$ for all $k \geq 0$, we have

$$\sum_{k=k_0}^{\infty} \sum_{j=0}^{N(d,k)} \frac{\alpha_{k,j}^2}{\lambda_k^{\text{FC}_\beta(2)}} \leq \sum_{k=k_0}^{\infty} \sum_{j=0}^{N(d,k)} \frac{1}{C_1} k^d \alpha_{k,j}^2 = \frac{B_2}{C_1} \sum_{k=k_0}^{\infty} \sum_{j=0}^{N(d,k)} \frac{1}{B_2} k^d \alpha_{k,j}^2 < \infty,$$

implying that $\|f\|_{\mathcal{H}^{\text{FC}_\beta(2)}}^2 < \infty$, and so $\mathcal{H}^{\text{Lap}} \subseteq \mathcal{H}^{\text{FC}_\beta(2)}$. Similar arguments can be used to show that $\mathcal{H}^{\text{FC}_\beta(2)} \subseteq \mathcal{H}^{\text{Lap}}$, proving that $\mathcal{H}^{\text{FC}_\beta(2)} = \mathcal{H}^{\text{Lap}}$. Finally, following the inclusion relation (12) the theorem is proved. \square

D NTK in \mathbb{R}^d

In this section we denote $r_x = \|\mathbf{x}\|$, $r_z = \|\mathbf{z}\|$ and by $\hat{\mathbf{x}} = \mathbf{x}/r_x$, $\hat{\mathbf{z}} = \mathbf{z}/r_z$. We first prove Theorem 9 and as a consequence Lemma 8 is proved.

Theorem 9. Let $\mathbf{k}^{\text{FC}_0(L)}(\mathbf{x}, \mathbf{z})$, $\mathbf{k}^{\text{FC}_\beta(L)}(\mathbf{x}, \mathbf{z})$, $\mathbf{x}, \mathbf{z} \in \mathbb{R}^d$, denote the NTK kernel with L layers without bias and with bias initialized at zero, respectively. It holds that (1) Bias-free $\mathbf{k}^{\text{FC}_0(L)}$ is homogeneous of order 1. (2) Let $\mathbf{k}^{\text{Bias}(L)} = \mathbf{k}^{\text{FC}_\beta(L)} - \mathbf{k}^{\text{FC}_0(L)}$. Then, $\mathbf{k}^{\text{Bias}(L)}$ is homogeneous of order 0.

Lemma 8. Let $\mathbf{k}^{\text{FC}_\beta(L)}(\mathbf{x}, \mathbf{z})$, $\mathbf{x}, \mathbf{z} \in \mathbb{S}^{d-1}$, denote the NTK kernels for FC networks with $L \geq 2$ layers, possibly with bias initialized with zero. This kernel is zonal, i.e., $\mathbf{k}^{\text{FC}_\beta(L)}(\mathbf{x}, \mathbf{z}) = \mathbf{k}^{\text{FC}_\beta(L)}(\mathbf{x}^T \mathbf{z})$.

To that end, we first prove the following supporting Lemma.

Lemma 9. For $\mathbf{x}, \mathbf{z} \in \mathbb{R}^d$ it holds that

$$\Theta^{(L)}(\mathbf{x}, \mathbf{z}) = r_x r_z \Theta^{(L)}(\hat{\mathbf{x}}, \hat{\mathbf{z}}) = r_x r_z \Theta^{(L)}(\hat{\mathbf{x}}^T \hat{\mathbf{z}}),$$

where $\Theta^{(L)} = \mathbf{k}^{\text{FC}_0(L+1)}$, as defined in Appendix A.

Proof. We prove this by induction over the recursive definition of $\mathbf{k}^{\text{FC}_0(L+1)} = \Theta^{(L)}(\mathbf{x}, \mathbf{z})$. Let $\mathbf{x}, \mathbf{z} \in \mathbb{R}^d$, then by definition

$$\Theta^{(0)}(\mathbf{x}, \mathbf{z}) = \mathbf{x}^T \mathbf{z} = r_x r_z \Theta^{(0)}(\hat{\mathbf{x}}, \hat{\mathbf{z}}) = r_x r_z \Theta^{(0)}(\hat{\mathbf{x}}^T \hat{\mathbf{z}})$$

and

$$\Sigma^{(0)}(\mathbf{x}, \mathbf{z}) = \mathbf{x}^T \mathbf{z} = r_x r_z \Sigma^{(0)}(\hat{\mathbf{x}}, \hat{\mathbf{z}}) = r_x r_z \Sigma^{(0)}(\hat{\mathbf{x}}^T \hat{\mathbf{z}})$$

Assuming the induction hypothesis holds for l , i.e.,

$$\Theta^{(l)}(\mathbf{x}, \mathbf{z}) = r_x r_z \Theta^{(l)}(\hat{\mathbf{x}}, \hat{\mathbf{z}}) = r_x r_z \Theta^{(l)}(\hat{\mathbf{x}}^T \hat{\mathbf{z}})$$

and

$$\Sigma^{(l)}(\mathbf{x}, \mathbf{z}) = r_x r_z \Sigma^{(l)}(\hat{\mathbf{x}}, \hat{\mathbf{z}}) = r_x r_z \Sigma^{(l)}(\hat{\mathbf{x}}^T \hat{\mathbf{z}})$$

we prove that those equalities are also true for $l+1$.

By the definition of $\lambda^{(l)}$ (6) and the induction hypothesis for $\Sigma^{(l)}$ we have that

$$\lambda^{(l)}(\mathbf{x}, \mathbf{z}) = \frac{\Sigma^{(l)}(\mathbf{x}, \mathbf{z})}{\sqrt{\Sigma^{(l)}(\mathbf{x}, \mathbf{x}) \Sigma^{(l)}(\mathbf{z}, \mathbf{z})}} = \frac{\Sigma^{(l)}(\hat{\mathbf{x}}, \hat{\mathbf{z}})}{\sqrt{\Sigma^{(l)}(\hat{\mathbf{x}}, \hat{\mathbf{x}}) \Sigma^{(l)}(\hat{\mathbf{z}}, \hat{\mathbf{z}})}} = \lambda^{(l)}(\hat{\mathbf{x}}, \hat{\mathbf{z}}) = \lambda^{(l)}(\hat{\mathbf{x}}^T \hat{\mathbf{z}})$$

Plugging this result in the definitions of Σ (7) and $\dot{\Sigma}$ (8), using the induction hypothesis we obtain

$$\begin{aligned}\Sigma^{(l+1)}(\mathbf{x}, \mathbf{z}) &= r_x r_z \Sigma^{(l+1)}(\hat{\mathbf{x}}, \hat{\mathbf{z}}) = r_x r_z \Sigma^{(l+1)}(\hat{\mathbf{x}}^T \hat{\mathbf{z}}) \\ \dot{\Sigma}^{(l+1)}(\mathbf{x}, \mathbf{z}) &= \dot{\Sigma}^{(l+1)}(\hat{\mathbf{x}}, \hat{\mathbf{z}}) = \dot{\Sigma}^{(l+1)}(\hat{\mathbf{x}}^T \hat{\mathbf{z}})\end{aligned}\quad (19)$$

Finally, using the recursion formula (5) ($\beta = 0$) and the induction hypothesis for $\Theta^{(l)}$, we obtain

$$\Theta^{(l+1)}(\mathbf{x}, \mathbf{z}) = r_x r_z \Theta^{(l+1)}(\hat{\mathbf{x}}, \hat{\mathbf{z}}) = r_x r_z \Theta^{(l+1)}(\hat{\mathbf{x}}^T \hat{\mathbf{z}})$$

□

A corollary of this Lemma is that $\mathbf{k}^{\text{FC}_0(\text{L})}$ is homogeneous of order 1 in \mathbb{R}^d , proving the first part of Theorem 9. Also, it is homogeneous of order 0 in \mathbb{S}^{d-1} , proving Lemma 8 for $\beta = 0$.

We next turn to proving the second part of Theorem 9, i.e., that $\mathbf{k}^{\text{Bias}(\text{L})} = \mathbf{k}^{\text{FC}_\beta(\text{L})} - \mathbf{k}^{\text{FC}_0(\text{L})}$ is homogeneous of order 0 in \mathbb{R}^d . By rewriting the recursive definition of $\mathbf{k}^{\text{FC}_\beta(\text{L})}$, shown in Appendix A, we can express $\mathbf{k}^{\text{Bias}(\text{L})}$ in the following recursive manner $\mathbf{k}^{\text{Bias}(1)} = \beta^2$, and $\mathbf{k}^{\text{Bias}(l+1)} = \mathbf{k}^{\text{Bias}(l)} \dot{\Sigma} + \beta^2$. Therefore, $\mathbf{k}^{\text{Bias}(\text{L})}$ is homogeneous of order zero, since it depends only on $\dot{\Sigma}$, which is by itself homogeneous of order zero (19). This concludes Theorem 9.

Finally, Lemma 8 is proved, since $\mathbf{k}^{\text{FC}_\beta(\text{L})} = \mathbf{k}^{\text{FC}_0(\text{L})} + \mathbf{k}^{\text{Bias}(\text{L})}$, and when restricted to \mathbb{S}^{d-1} both components are homogeneous of order 0.

Theorem 10. *Let $p(r)$ be a decaying density on $[0, \infty)$ such that $0 < \int_0^\infty p(r) r^2 dr < \infty$ and $\mathbf{x}, \mathbf{z} \in \mathbb{R}^d$.*

1. *Let $\mathbf{k}_0(\mathbf{x}, \mathbf{z})$ be homogeneous of order 1 such that $\mathbf{k}_0(\mathbf{x}, \mathbf{z}) = r_x r_z \hat{\mathbf{k}}_0(\hat{\mathbf{x}}^T \hat{\mathbf{z}})$. Then its eigenfunctions with respect to $p(r_x)$ are given by $\Psi_{k,j} = a r_x Y_{k,j}(\hat{\mathbf{x}})$, where $Y_{k,j}$ are the spherical harmonics in \mathbb{S}^{d-1} and $a \in \mathbb{R}$.*
2. *Let $\mathbf{k}(\mathbf{x}, \mathbf{z}) = \mathbf{k}_0(\mathbf{x}, \mathbf{z}) + \mathbf{k}_1(\mathbf{x}, \mathbf{z})$ so that \mathbf{k}_0 as in 1 and \mathbf{k}_1 is homogeneous of order 0. Then the eigenfunctions of \mathbf{k} are of the form $\Psi_{k,j} = (a r_x + b) Y_{k,j}(\hat{\mathbf{x}})$.*

Proof. 1. Since $\hat{\mathbf{k}}_0$ is zonal, its Mercer's representation reads

$$\hat{\mathbf{k}}_0(\hat{\mathbf{x}}, \hat{\mathbf{z}}) = \sum_{k=0}^{\infty} \lambda_k \sum_{j=1}^{N(d,k)} Y_{k,j}(\hat{\mathbf{x}}) Y_{k,j}(\hat{\mathbf{z}}),$$

where the spherical harmonics $Y_{k,j}$ are the eigenfunctions of $\hat{\mathbf{k}}_0$. Consequently, as noted also in [12],

$$\mathbf{k}_0(\mathbf{x}, \mathbf{z}) = a^2 \sum_{k=0}^{\infty} \lambda_k \sum_{j=1}^{N(d,k)} r_x Y_{k,j}(\hat{\mathbf{x}}) r_z Y_{k,j}(\hat{\mathbf{z}}).$$

The orthogonality of the eigenfunctions $\Psi_{k,j}(\mathbf{x}) = a r_x Y_{k,j}(\hat{\mathbf{x}})$ is verified as follows. Let $\bar{p}(\mathbf{x})$ denote a probability density on \mathbb{R}^d such that $\bar{p}(\mathbf{x}) = p(r_x)/A(r_x)$, where $A(r_x)$ denotes the surface area of a sphere of radius r_x in \mathbb{R}^d . Then,

$$\int_{\mathbb{R}^d} \Psi_{k,j}(\mathbf{x}) \Psi_{k',j'}(\mathbf{x}) \bar{p}(\mathbf{x}) d\mathbf{x} = a^2 \int_0^\infty \frac{r_x^{d+1} p(r_x)}{A(r_x)} dr_x \int_{\mathbb{S}^{d-1}} Y_{k,j}(\hat{\mathbf{x}}) Y_{k',j'}(\hat{\mathbf{x}}) d\hat{\mathbf{x}} = \delta_{k,k'} \delta_{j,j'},$$

where the rightmost equality is due to the orthogonality of the spherical harmonics and by setting

$$a^2 = \left(\int_0^\infty \frac{r_x^{d+1} p(r_x)}{A(r_x)} dr_x \right)^{-1}.$$

Clearly this integral is positive, and the conditions of the theorem guarantee that it is finite.

2. By the conditions of the theorem we can write

$$\mathbf{k}(\mathbf{x}, \mathbf{z}) = r_x r_z \hat{\mathbf{k}}_0(\hat{\mathbf{x}}^T \hat{\mathbf{z}}) + \hat{\mathbf{k}}_1(\hat{\mathbf{x}}^T \hat{\mathbf{z}}),$$

where $\hat{\mathbf{x}}, \hat{\mathbf{z}} \in \mathbb{S}^{d-1}$. On the hypersphere the spherical harmonics are the eigenfunctions of \mathbf{k}_0 and \mathbf{k}_1 . Denote their eigenvalues respectively by λ_k and μ_k , so that

$$\int_{\mathbb{S}^{d-1}} \mathbf{k}_0(\hat{\mathbf{x}}^T \hat{\mathbf{z}}) \bar{Y}_k(\hat{\mathbf{z}}) d\hat{\mathbf{z}} = \lambda_k \bar{Y}_k(\hat{\mathbf{x}}) \quad (20)$$

$$\int_{\mathbb{S}^{d-1}} \mathbf{k}_1(\hat{\mathbf{x}}^T \hat{\mathbf{z}}) \bar{Y}_k(\hat{\mathbf{z}}) d\hat{\mathbf{z}} = \mu_k \bar{Y}_k(\hat{\mathbf{x}}), \quad (21)$$

where $\bar{Y}_k(\hat{\mathbf{x}})$ denote the zonal spherical harmonics. We next show that the space spanned by the functions $r_x \bar{Y}_k(\mathbf{x})$ and $\bar{Y}_k(\mathbf{x})$ is fixed under the following integral transform

$$\int_{\mathbb{R}^d} \mathbf{k}(\mathbf{x}, \mathbf{z}) (\alpha r_z + \beta) \bar{Y}_k(\hat{\mathbf{z}}) \bar{p}(\mathbf{z}) d\mathbf{z} = (a r_x + b) \bar{Y}_k(\hat{\mathbf{x}}), \quad (22)$$

$\alpha, \beta, a, b \in \mathbb{R}$ are constants. The left hand side can be written as the application of an integral operator $T(\mathbf{x}, \mathbf{z})$ to a function $\Phi_{\alpha, \beta}^k(\mathbf{z}) = (\alpha r_z + \beta) \bar{Y}_k(\hat{\mathbf{z}})$. Expressing this operator application in spherical coordinates yields

$$T(\mathbf{x}, \mathbf{z}) \Phi_{\alpha, \beta}^k(\mathbf{z}) = \int_0^\infty \frac{p(r_z) r_z^{d-1}}{A(r_z)} dr_z \int_{\hat{\mathbf{z}} \in \mathbb{S}^{d-1}} (r_x r_z \mathbf{k}_0(\hat{\mathbf{x}}^T \hat{\mathbf{z}}) + \mathbf{k}_1(\hat{\mathbf{x}}^T \hat{\mathbf{z}})) (\alpha r_z + \beta) \bar{Y}_k(\hat{\mathbf{z}}) d\hat{\mathbf{z}}.$$

We use (20) and (21) to substitute for the inner integral, obtaining

$$T(\mathbf{x}, \mathbf{z}) \Phi_{\alpha, \beta}^k(\mathbf{z}) = \int_0^\infty \frac{p(r_z) r_z^{d-1}}{A(r_z)} (\lambda_k r_x r_z + \mu_k) (\alpha r_z + \beta) \bar{Y}_k(\hat{\mathbf{x}}) dr_z.$$

Together with (22), this can be written as

$$T(\mathbf{x}, \mathbf{z}) \Phi_{\alpha, \beta}(\mathbf{z}) = \Phi_{a, b}(\mathbf{x}),$$

where

$$\begin{pmatrix} a \\ b \end{pmatrix} = \begin{pmatrix} \lambda_k & 0 \\ 0 & \mu_k \end{pmatrix} \begin{pmatrix} M_2 & M_1 \\ M_1 & M_0 \end{pmatrix} \begin{pmatrix} \alpha \\ \beta \end{pmatrix}$$

where $M_q = \int_0^\infty \frac{r_z^{q+d-1} p(r_z)}{A(r_z)} dr_z$, $0 \leq q \leq 2$. By the conditions of the theorem these moments are finite. This proves that the space spanned by $\{r_x \bar{Y}(\hat{\mathbf{x}}), \bar{Y}(\hat{\mathbf{x}})\}$ is fixed under $T(\mathbf{x}, \mathbf{z})$, and therefore the eigenfunctions of $\mathbf{k}^{\text{FC}_\beta(\text{L})}(\mathbf{x}, \mathbf{z})$ take the form $(\bar{a} r_x + \bar{b}) \bar{Y}(\hat{\mathbf{x}})$ for some constants \bar{a}, \bar{b} . □

The implication of Theorem 10 is that the eigenvectors of $\mathbf{k}^{\text{FC}_0(\text{L})}$ are the spherical harmonic functions, scaled by the norm of their arguments. With bias, $\mathbf{k}^{\text{FC}_\beta(\text{L})}$ has up to $2N(d, k)$ eigenfunctions for every frequency k , of the general form $(a r_x + b) \bar{Y}_{k, j}(\hat{\mathbf{x}})$ where a, b are constants that differ from one eigenfunction to the next.

E Experimental Details

E.1 The UCI dataSet

In this section, we provide experimental details for the UCI dataset. We use precisely the same pre-processed datasets, and follow the same performance comparison protocol as in [4].

NTK Specifications We reproduced the results of [4] using the publicly available code¹, and followed the same protocol as in [4]. The total number of kernels evaluated in [4] are 15 and the SVM cost value parameter \mathbf{C} is tuned from 10^{-2} to 10^4 by powers of 10. Hence, the total number of hyper-parameter combinations searched using cross-validation is 105 (15×7).

¹<https://github.com/LeoYu/neural-tangent-kernel-UCI>

Exponential Kernels Specifications For the Laplace and Gaussian kernels, we searched for 10 kernel bandwidth values ($1/c$) from $2^{-2} \times \nu$ to ν in the log space with base 2, where ν is chosen heuristically as the median of pairwise l_2 distances between data points (known as the *median trick* [19]). So, the total number of kernel evaluations is 10. For γ -exponential, we searched through 5 equally spaced values of γ from 0.5 to 2. Since we wanted to keep the number of the kernel evaluations the same as for NTK in [4], we searched through only three kernel bandwidth values ($1/c$) which are 1, ν and #features (default value in the **sklearn** package²). So, the total number of kernel evaluations is 15 (5×3).

For a fair comparison with [4], we swept the same range of SVM cost value parameter **C** as in [4], i.e., from 10^{-2} to 10^4 by powers of 10. Hence, the total number of hyper-parameter search using cross-validation is 70 (10×7) for Laplace and 105 (15×7) for γ -exponential which is the same as for NTK in [4].

E.2 Large scale datasets

We used the experimental setup mentioned in [41] and the publicly available code³. [41] solves kernel ridge regression (KRR [43]) using the FALKON algorithm, which solves the following linear system

$$(K_{nn} + \lambda nI) \alpha = \hat{\mathbf{y}},$$

where K is an $n \times n$ kernel matrix defined by $(K)_{ij} = K(x_i, x_j)$, $\hat{\mathbf{y}} = (y_1, \dots, y_n)^T$, and λ is the regularization parameter. Refer to [41] for more details.

In Table 4, we provide the hyper parameters chosen with cross validation.

	MillionSongs [11]	SUSY [39]	HIGGS [39]
H- γ -exp.	$\gamma = 1.4, \sigma = 5, \lambda = 1e^{-6}$	$\gamma = 1.8, \sigma = 5, \lambda = 1e^{-7}$	$\gamma = 1.6, \sigma = 8, \lambda = 1e^{-8}$
H-Laplace	$\sigma = 3, \lambda = 1e^{-6}$	$\sigma = 4, \lambda = 1e^{-7}$	$\sigma = 8, \lambda = 1e^{-8}$
NTK	$L = 9, \lambda = 1e^{-9}$	$L = 3, \lambda = 1e^{-8}$	$L = 3, \lambda = 1e^{-6}$
H-Gaussian	$\sigma = 8, \lambda = 1e^{-6}$	$\sigma = 3, \lambda = 1e^{-7}$	$\sigma = 8, \lambda = 1e^{-8}$

Table 4: Hyper-parameters chosen with cross validation for the different kernels.

E.3 C-Exp: Convolutional Exponential Kernels

Let $\mathbf{x} = (x_1, \dots, x_d)^T$ and $\mathbf{z} = (z_1, \dots, z_d)^T$ denote two vectorized images. Let P denote a window function (we used 3×3 windows). Our hierarchical exponential kernels are defined by $\Theta(\mathbf{x}, \mathbf{z})$ as follows:

$$\begin{aligned}
\Theta_{ij}^{[0]}(\mathbf{x}, \mathbf{z}) &= x_i z_j \\
s_{ij}^{[h]}(\mathbf{x}, \mathbf{z}) &= \sum_{m \in P} \Theta^{[h]}(x_{i+m}, z_{j+m}) + \beta^2 \\
\Theta_{ij}^{[h+1]}(\mathbf{x}, \mathbf{z}) &= K(s_{ij}^{[h]}(\mathbf{x}, \mathbf{z}), s_{ii}^{[h]}(\mathbf{x}, \mathbf{x}), s_{jj}^{[h]}(\mathbf{z}, \mathbf{z})) \\
\bar{\Theta}(\mathbf{x}, \mathbf{z}) &= \sum_i \Theta_{ii}^{[L]}(\mathbf{x}, \mathbf{z})
\end{aligned}$$

where $\beta \geq 0$ denotes the bias and the last step is analogous to a fully connected layer in networks, and we set

$$K(s_{ij}, s_{ii}, s_{jj}) = \sqrt{s_{ii}s_{jj}} \mathbf{k} \left(\frac{s_{ij}}{\sqrt{s_{ii}s_{jj}}} \right)$$

where \mathbf{k} can be any kernel defined on the sphere. In the experiments we applied this scheme to the three exponential kernels, Laplace, Gaussian and γ -exponential.

²https://scikit-learn.org/stable/modules/generated/sklearn.metrics.pairwise.rbf_kernel.html

³https://github.com/LCSL/FALKON_paper

Technical details We used the following four kernels:

CNTK [2] $L = 6, \beta = 3$.

C-Exp Laplace. $L = 3, \beta = 9, \mathbf{k}(\mathbf{x}^T \mathbf{z}) = a + be^{-c\sqrt{2-2\mathbf{x}^T \mathbf{z}}}$ with $a = -11.491, b = 12.606, c = 0.048$.

C-Exp γ -exponential. $L = 8, \beta = 3, \mathbf{k}(\mathbf{x}^T \mathbf{z}) = a + be^{-c(2-2\mathbf{x}^T \mathbf{z})^{\gamma/2}}$ with $a = -0.276, b = 1.236, c = 0.424, \gamma = 1.888$.

C-Exp Gaussian. $L = 12, \beta = 3, \mathbf{k}(\mathbf{x}^T \mathbf{z}) = a + be^{-c(2-2\mathbf{x}^T \mathbf{z})}$ with $a = -0.22, b = 1.166, c = 0.435$.

For each kernel \mathbf{k} above, the parameters a, b, c and γ were chosen using non-linear least squares optimization with the objective $\sum_{u \in U} (\mathbf{k}(u) - \mathbf{k}^{\text{FC}_{\beta}(2)}(u))^2$, where $\mathbf{k}^{\text{FC}_{\beta}(2)}$ is the NTK for a two-layer network defined in (9) with bias $\beta = 1$, and the set U included (inner products between) pairs of normalized $3 \times 3 \times 3$ patches drawn uniformly from the CIFAR images. The number of layers L is chosen by cross validation.

For the training phase we used 1-hot vectors from which we subtracted 0.1, as in [38]. For the classification phase, as in [30], we normalized the kernel matrices such that all the diagonal elements are ones. To avoid ill conditioned kernel matrices we applied ridge regression with a regularization factor of $\lambda = 5 \cdot 10^{-5}$. Finally, to reduce overall running times, we parallelized the kernel computations on NVIDIA Tesla V100 GPUs.